8-2017

Simulation Modeling Approach for Evaluating a Solution Designed to Alleviate the Congestion of Passenger Flow at the Composure Area of Security Checkpoints

Maria Luisa Janer Rubio
University of Arkansas, Fayetteville

Simulation Modeling Approach for Evaluating a Solution Designed to Alleviate the Congestion of Passenger Flow at the Composure Area of Security Checkpoints

A thesis submitted in partial fulfillment
of the requirements for the degree of
Master of Science in Industrial Engineering

by

Maria Luisa Janer Rubio
University of Arkansas
Bachelor of Science in Industrial Engineering, 2015

August 2017
University of Arkansas

This thesis is approved for recommendation to the Graduate Council.

Dr. Manuel Rossetti
Thesis Director

Dr. Richard Ham
Committee Member

Dr. Shengfan Zhang
Committee Member

Abstract

In a previous study, we found that replacing the exit roller of a security checkpoint lane for a continuously circulating conveyor could potentially increase the throughput of passengers by over 28% while maintaining the TSA security-waiting time limit (Janer and Rossetti 2016). This study intends to expand this previous effort by investigating the impact of this circulating conveyor on the secondary screening related processes. Leone and Liu (2011) found that imposing a limit on the x-ray screening time, and diverting any item exceeding this limit to secondary screening, could decrease the waiting time by 43%. Our objective is to verify Leone and Lui's findings using discrete event simulation, and evaluate the effect of a circulating conveyor on these findings. In particular, we intend to optimize univariate response curves of the same response variable in Leone and Liu's effort. Simulation will be used to evaluate the optimal solution, and investigate the possibility of replacing a traditional two-lane system with a single lane having the circulating conveyor in place.

Acknowledgements

I extend a special thanks to my faculty advisor, Dr. Manuel Rossetti, for his support, time and long hours invested on this study. It could not have been possible without you.

Table of Contents

List of Figures

List of Exhibits

List of Tables

I. INTRODUCTION

As the world has progressively transformed into an integrated global economy, air transportation has become one of the most fundamental means to connect people in distant places. Revenue Passenger Miles (RPMs) is the aviation standard for measuring air travel volume. It represents one paying passenger travelling one mile. The U.S. Department of Transportation’s Federal Aviation Administration’s (FAA) projected in 2013 that U.S. carriers RPMs will grow 76% by 2034, and the number of people flying per year will increase from 745.5 million in 2014 to 1.15 billion in 2034 (Price 2014).

One of the major concerns is the U.S. airports’ infrastructure available to sustain this growth. Prior to September 11, 2001, there was no concrete process to screen checked luggage. In fact, only 5% of the checked bags were investigated (Blalock 2007). In 2002, the Transportation Security Administration (TSA) mandated to begin screening 100% of the checked luggage (Mead 2003). This involved installing explosive detection system machines of the size of sport utility vehicles and massive conveyor systems across all U.S. commercial airports (Blalock 2007). This left very little space to accommodate passenger screening procedures, and possible future growth of passenger traffic. Consequently, passenger-screening operations have become one of the major bottlenecks among airport operations today (Blalock 2007).

In an effort to provide solutions to the major causes of constrained flow, several studies have identified the x-ray as the main impediment of continuous traffic of passengers and items (De Barros and Tomber 2007). A study performed at the Dallas/Fort Worth International Airport (DFW) attributed this to the processes of divestiture and composure, happening before and after the x-ray, respectively (DFW Planning Department 2005). Regarding divestiture, the problem resides with passengers waiting until they have reached the divestiture tables to start preparing for screening. In addition, once they are in the divestiture area, they fail to remove the required items from their luggage or person. Regarding composure, some passengers are delayed by a second security officer after they pass through the body scanner. As a result, their bags may be delivered to the exit roller before they have completed their body screening. These bags will be blocking the bags of the following passenger, who may finish screening before the passenger who was delayed. In addition, passengers fail to move to the designated benches to put their items back in their carry-on luggage. Instead, they remain in the exit roller area. Both of these issues contribute to interrupting the x-ray operation, because often there is not enough space on the exit roller to continue delivering items to the cleared passengers (DFW Planning Department 2005).

The TSA as well as several airlines have taken several measures to avoid some of this inconvenience. Divestiture officers have been implemented to educate passengers during the divestiture process. Moreover, additional officers are employed during peak seasons of the year at major hub airports to instruct passengers to start divesting while they are waiting in line. Studies have shown that airports providing instruction to passengers during the divestiture stage increase their average throughput by 9% as x-ray operators are less likely to repeat the screening of a bag for divestiture failures (Passenger Facilitation 2011). In addition, in May 2016, Delta Air Lines inaugurated a pair of automated lanes at Hartsfield-Jackson Atlanta International Airport (ATL). These lanes enable parallel processing of five passengers during divestiture. Moreover, an automated bin system returns empty trays to passengers divesting. In addition, if a suspicious item is detected, the bin or carry-on item is diverted to secondary screening without interrupting the x-ray operation. The system was implemented in November 2016 at Chicago O'Hare Airport (ORD), and it is under implementation at DFW, San Francisco International

Airport (SFO) and Los Angeles International Airport (LAX) (Solomon 2016). Similarly, the Pre-Check program, introduced in 2013, is increasingly growing. It was established to improve the experience and security benefit of known travelers and the overall checkpoint performance. As of September 2015, 1.6 million individuals have enrolled, and the TSA estimates the number could rise to 25 million by 2020 if they focus the program marketing on the private sector (TSA Pre-Check Expansion Act 2016).

Despite these improvements, the long waiting lines remain a concern, especially for the peak seasons of the year. In 2016, the TSA experienced a shortage of screeners as they reduced the staff by 12% since 2013 due to federal budget cuts. On the other hand, summer passenger traffic has increased by 15% since the summer of 2013 (Davis 2016). Consequently, in May 2016, passengers experienced waiting times of up to 50 minutes in major airports, including DFW, SFO and ATL. As a result, the TSA employed private security screeners, and intensified the use of security dogs to aid the screening of passengers for the rest of the summer (Quintana and Sze 2016).

This research aims to evaluate a solution designed to alleviate the long waiting lines caused by seasonal travelers. We address specifically the issues at composure where some passengers can block the way of other passengers if they are delayed after the body screening. We investigate the possibility of implementing a continuously circulating conveyor on place of the exit roller of one of the checkpoint lanes. We use discrete event simulation (DES) to evaluate the effect of this circulating conveyor on the x-ray screening and secondary manual screening. We use the professional version 15 of Arena Rockwell Software as the simulation software of this study.

This paper is organized as follows: in Section 2, we review the efforts found in the literature on improving the performance of security checkpoints using DES or analytics. In Section 3, we describe in detail the system under study, and the solution prototypes. In Section 4, we illustrate the conceptual modeling, and the key constructs used to implement the simulation models. In Section 5, we summarize the efforts used to obtain the distribution parameters for the models. In Section 6, we explain in detail how we verified and validated the models. In Section 7, we explain the experimentation methods and results obtained from evaluating the models.

II. LITERATURE REVIEW

As we are trying to evaluate a solution that can benefit both the security of passengers and the passenger flow, we reviewed studies focusing on both or either of these two aspects. Several studies concentrate on diagnosing causes of passenger flow congestion or investigating the interrelation between variables having an effect on the checkpoint throughput performance. De Barros and Tomber (2007) evaluated and quantified the impact of post 9/11 security measures on the planning and operations of airport terminals. They built a spreadsheet model based on deterministic querying theory to obtain estimates of the queue length and approximate waiting times at the passenger screening. Moreover, they used a simulation model built in Arena to evaluate seven scenarios associated with the different measures implemented after 9/11. Their findings assert that reducing the number of carry-on items to one item per passenger was the most effective measure to reduce the waiting time of passengers. In addition, adding pre-screening tables for passengers to divest helped reducing the waiting time by almost two thirds. Moreover, they compare the different methods available to analyze security checkpoints. As they explain, in the absence of data, a mathematical model can provide meaningful insights about the interrelationships between variables and service components. Despite this contribution, they fail to explain their definition for waiting time. In addition, it is impossible to qualify their models as realistic as they provide no detail about the assumptions made to implement the analytic and simulation models.

Similar to De Barros and Tomber, Dorton and Liu (2016) used an analytical model based on queuing theory, and an empirical approach using DES to evaluate the effects of baggage volume (number of items per passenger) and alarm rate on the cycle time and passenger throughput. For the theoretical approach, they define alarm rate as the probability of a bag being cleared from screening. They conclude that the queueing network approach can accurately represent the real system when it is subject to steady-state assumptions. Otherwise, several of these assumptions do not apply to the real system. Different from the theoretical approach, they define alarm rate as the probability of a passenger being cleared from screening for the empirical approach. In other words, they eliminate the effect of the baggage volume on alarm rate, and they fail to make the necessary adjustments to the parameters to make such an assumption. Consequently, using DES, they found that alarm rate highly affects the cycle time and passenger throughput, while baggage volume slightly affects cycle time, and has no effect on throughput. Moreover, one of their assumptions for the DES states that the travel document check (TDC) process was ignored. However, to evaluate the sensitivity of cycle time to alarm rate and baggage volume, they take into consideration the TSA standard limit of ten minutes, which does include the TDC processing time (TSA Checkpoint Design Guide Revision 5.1 2014). Our study will explore the effect of baggage volume on alarm rate by building upon the input parameters of Dolton and Liu's study. In addition, we will model the TDC as one of the processes considered within the TSA system time limit.

Doran, Gokhale and Lownes (2013) proposed an analytic model consisting of various service components to estimate the time it takes passengers to pass through security checkpoints. The model intends to illustrate how the standard security checkpoint end-to-end completion time is affected by the variability in service time of the different service components, the different profiles of passenger types, and the policies of the physical configuration. They use hyper-exponential distributions for each service component in order to model service times exhibiting a coefficient of variation larger than one. They use a discrete-time Markov chain to model the probabilistic flow of passengers among the service components. Then, they model the various passenger profiles by decreasing or increasing the means of the hyper-exponential distributions in every service component by a certain percentage. However, they fail to indicate where they obtain the values of the percentages used in the experiments. In addition, they do not provide enough detail in regards to the validity of their assumptions or model. Lastly, they model a two-lane system with three TDC stations. The TSA Checkpoint Design Guide mandates that there should be one TDC station for every two-lane passenger screening system (2014).

Wetter, Lipphardt and Hofer (2011) performed an exploratory analysis on the influence of different factors on throughput, cycle time and passenger density (number of passengers simultaneously at the checkpoint) as well as on subjective performance measures collected from surveying the security officers, including work strain, work satisfaction, and overall checkpoint performance. The study was carried out from October 2008 to October 2009 at two separate docks of a large European airport serving as an airline hub. One of the docks featured a "traditional" layout having a single lane with one walk-through medal detector (WTMD). The other dock featured a "mirror" layout with two lanes sharing a WTMD. They evaluated the effect of seasonal temperature differences, the number of manual baggage inspections and different allocations of tasks among the security officers. They found the throughput to be highly sensitive to day temperature and to the number of manual baggage inspections. In addition, they found that taking away the divestiture officer and assigning him as second person for manual baggage checks increased the number of manual baggage checks and the frequency of metal alarms from the WTMD. Consequently, this intensified the work strain for security officers, but, surprisingly, it increased throughput by around 18% in both of the docks. They found no conclusive evidence to recommend one of the two checkpoint layouts studied. However, they found the "mirror" layout to have more flexibility with respect to the WTMD officers. They claim that the layout allows a security officer to switch actively between helping at the WTMD and working as a second person for manual baggage checks. In addition, the layout only requires a single WTMD and less space than the "traditional" layout. Life testing observations can give meaningful insights about possible new aspects to take into consideration. Nonetheless, they can be very time consuming, and it is difficult to draw definite conclusions from them, as one does not have control over all the factors influencing the observations. It is often more recommended to collect enough data on all the possible aspects of interest. Then, construct a simulation model that contains reasonable ranges of parameters, and allow testing the effect of each factor individually.

Paul et al. (2009) developed a regression model to predict the passenger waiting time based on the number of open lanes, the average number of passengers processed per lane and the number of bins and carry-on items per passenger. They use a generic simulation model and a factorial design of experiments to estimate the coefficients of the regression model. Different from most of the studies reviewed, for this study extensive on-site data collection was performed. From analyzing this data, they found that x-ray processing times were lower for high-passenger-traffic hours and higher for low-passenger-traffic hours. They also found how the number of items per passenger vary significantly with time of the day and day of the week. They observed the highest number of items per passenger in the morning hours during weekdays, when most travelers are business passengers. In addition, the results of their simulation model show that the factors with highest impact on waiting time are passenger volume, number of items per passenger, number of lanes open and staff level. Their efforts on data collection will be summarized in Section 5.

Other studies were intended to develop templates to aid the simulation analysis of security checkpoint systems. Guru and Savory (2004) described their effort in developing an internet-based application to assist a simulation analyst in the conceptual modeling stage of security screening systems. The application consists of 15 templates of the security equipment, intended to help identify the important input modeling parameters, the system components and the interrelationships among the various components and parameters. Although the templates can give meaningful insights in regards to the security equipment, the study fails to illustrate how passengers, security officers, and the material handling are taken into account in their templates.

Fayetz et al. (2008) developed a decision support tool based on simulation designed to assess the current state of airports' functional areas as well as the impact of new procedures on space allocation per passenger and waiting times at the different processing points. The tool allows the modeling of new procedures by providing a simple framework to change the distribution parameters associated with each functional area. Thus, the tool can be very useful for evaluating small alterations for which one can instinctively predict the differences in the distribution. However, for more complex changes for which one cannot instinctively predict the differences in the distribution, it seems one must replicate the changes in real life in order to collect the data for the new input parameters, and have the tool accurately predict the impact of such changes.

Wilson, Roe and So (2006) present the Security Checkpoint Optimizer (SCO), a java-based DES tool developed by Northrop Group for the TSA. Similar to the tool presented by Fayetz et al., the SCO is spatially aware, and it was designed to evaluate passenger and lugagge throughput, security effectiveness, resource utilization and operational costs. Nonetheless, it contains a novel 2-D animation, enabling the user to verify the modeling of procedures implemented. In addition, it allows evaluating the security effectiveness by aggregating probabilities of detection for some item of interest.

Pendegraft, Robertson and Shrader (2004) present a DES model developed to evaluate new policies in the passenger and luggage screening systems at Baltimore Washington International Airport. Although they do not provide much detail in regards to the simulation model, they describe a step-by-step procedure for estimating arrival rate parameters from flight departure schedules. A detailed description of this contribution is presented in Section 5. In addition, they include the modeling of processes such as check-in and passenger boarding to represent accurately the impact that such processes have on the security checkpoint demand. The model was used to recommend resource requirements (x-rays, metal detectors, ETDs, and officers) in all the major hub airports in the United States.

Similar to our study, other efforts focus on proposing and evaluating the effectiveness of solutions to issues already identified. Leone and Liu (2011) observed that while 80% of the items are inspected within 7 seconds in the primary screening, a lengthy right tail in the distribution of the inspection time implies that a very small proportion of items are disproportionately contributing to decreasing the inspection rate and the overall checkpoint performance. They propose that imposing a limit in the primary screening inspection time and increasing the rejection rate to secondary screening of items taking longer than that limit would improve the throughput and overall waiting time of passengers. Using queuing and simulation models, they assert their solution decreases the mean waiting time by 43%, reduces the operation costs by 1%, and increases the probability of detecting a prohibited item to 10%. Nonetheless, it is not clear how obtain these two last conclusions, as they do not provide any detail about how they estimated operation costs and the probability of detecting a threat. Furthermore, similar to Dolton and Liu (2016), with their models, they obtain waiting times of above 12 minutes without modeling the TDC process. On the other hand, one contribution of this study is the detailed explanation on the data collection methods and parameters obtained for their models. This contribution will be discussed further in Section 5.

De Lange et al. (2013) investigate the possibility of implementing virtual queuing at security checkpoints by offering to some passengers a time window during which they can bypass the TDC queue, and have priority to access the security lanes. They implemented a DES model of a large international airport in Western Europe to determine whether virtual queueing could reduce the number of agents at security lanes while not increasing the average passenger waiting time. The essence of this solution consists of redistributing the passenger arrivals by shifting the checkpoint demand out of peak periods into de idle periods. They evaluated twelve different infinite horizon simulations of 100 days each to determine the optimal time window (TW) and the best time a passenger could be moved later in time (i.e. the best transfer time limit - TTL). Then, using the optimal TTL and TW, using four additional scenarios, they perform a sensitivity analysis on the participation level of passengers to determine the ultimate benefit of the solution. They conclude that the effectivity of the virtual queuing solution would depend on the reliability of the forecasting method, the arrival rate pattern, the number of eligible passengers, and the length of the TWs. They found that this solution works best for airports with arrival rate patterns displaying sharp and frequent peaks exceeding the checkpoint capacity, followed by periods of light passenger traffic. Considering virtual queuing allows reducing the number of security lanes required, they found that at least 60% of the eligible passengers must participate of the program to preserve the benefits of the solution. In addition, the TW should be kept as short as possible to maximize the transfer accuracy rate, as this ensures higher utilization of the idle capacity. Different from our study, De Lange et al. do not study the impact of the solution on security. Nonetheless, similar to our experiment design, their study consists of a series of sensitivity analysis on the input parameters of the solution.

The last set of reviewed studies provide some insights in regards to the assignment of passenger types based on the state of the system. Nie et al. (2011) investigate a solution to utilize effectively the Selectee Lane, which has more strict screening procedures than a normal lane, in order to maximize the probability of true alarm. They assume a prior prescreening process at the check-in assigns passengers into different risk classes according to the passengers' perceived risk levels. Consequently, they propose assigning the different risk classes to the Selectee Lane based on the number of passengers that are already in the lane. First, they study a steady-state model and formulate it as a nonlinear binary integer program. Next, they find an approximate solution to this model using a rule-based heuristic. Later, they explore the solution obtained using a simulation framework designed to evaluate different assignment solutions. Lastly, they use a neighborhood search procedure to derive assignment solutions with better performance from the initial heuristic solution, and evaluate the derived solutions using the simulation framework. The main contribution of this work to our study lays on the way the rule-based heuristic is formulated to guarantee solutions that maximize the objective of the study. For our purpose, we will formulate a similar rule-based heuristic to obtain an assignment solution that minimizes the passengers' waiting time. Nonetheless, Nie et al. do not provide any statistical support for their selection of running parameters for the simulation model. Moreover, it is not clear what type of horizon they use for their simulation framework.

III. SYSTEM DEFINITION

This section presents the system under study and the two prototypes of the solution that will be evaluated against the current configuration.

Our system consists of the passenger security-screening checkpoint, including passengers, security officers, material handling and security equipment. It extends from where passengers join a line to have their documents checked by a TDC officer until they have collected their last item from either the exit roller or the secondary screening station. The system is modeled according to the standards in the Revision 5.1 of the TSA Checkpoint Design Guide (2014). Figure 1 displays a layout of the system elements under study encircled in red.

Following advice from TSA design agents, we studied a two-lane mirror layout where two lanes share one WTMD, one advanced imaging technology (AIT) and one secondary screening station. Note we do not include in the system the Pre-Check lane, depicted above the dashed lane, or the processing of Pre-Check passengers.

Upon arrival, standard passengers join the queue for verifying their documents with a TDC officer. After the TDC officer has finished reviewing the passenger's documents, a different security officer directs the passenger to the lane with the smaller number of passengers waiting. There can be at most four passengers per lane waiting for divestiture. Thus, if there is not a space available in any of the two lanes, the passenger stays with the director officer until one space becomes available in either of two lanes. There can be at most two passenger waiting with the director security officer. Thus, when the system reaches this limit, the TDC officer stops processing passengers until space becomes available.

Next, passengers proceed to divestiture. Similar to what has been implemented in several major airports across the U.S., passengers proceed to one of five divestiture stations. Here they reach their trays from the tray return system below their divestiture stations. They take one tray at a time, load it, and push it to the roller conveyor taking the loaded items to the x-ray. The number of items that each passenger loads onto the conveyor varies according to a discrete random variable distribution. Further details on this distribution will be given in Section 5.

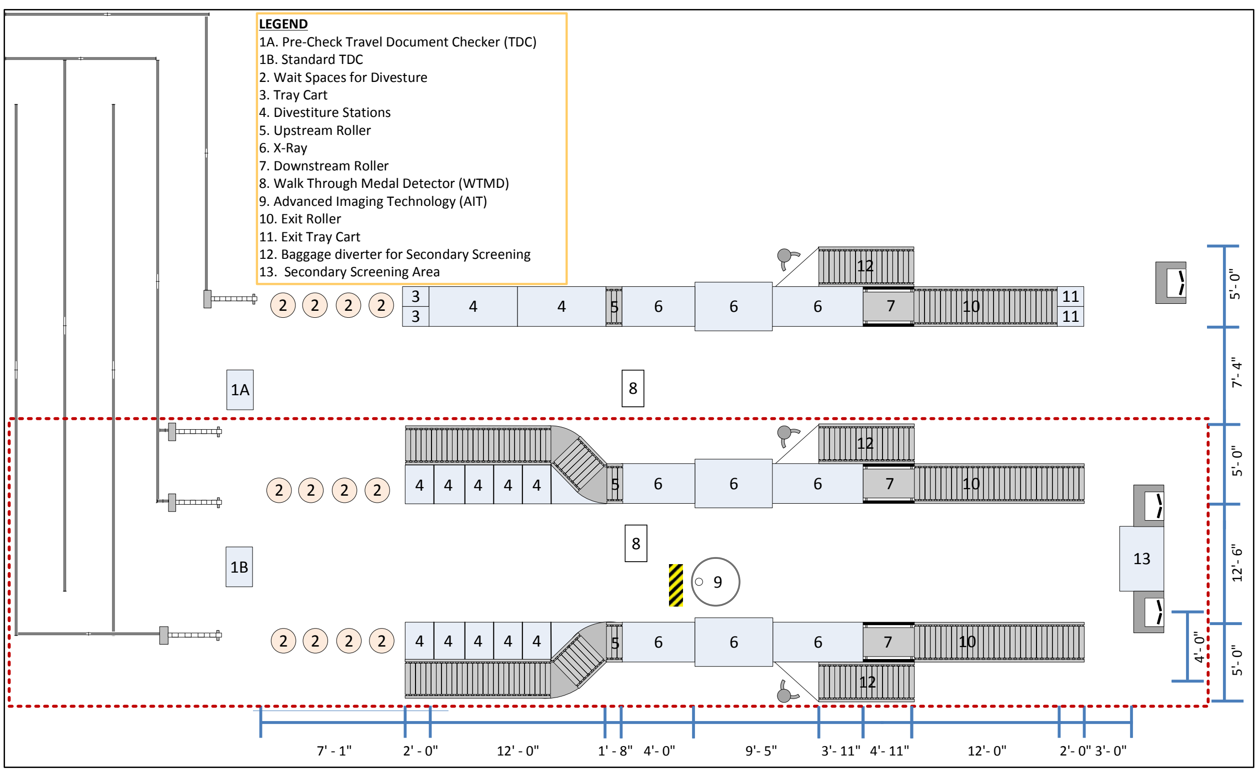

Figure 1. TSA Security Checkpoint Layout

After a passenger pushes his last item for screening, he proceeds to the AIT station while his items proceed to the x-ray, where items are processed individually. If a suspicious item is detected by the x-ray, the tray or carry-on item is automatically diverted to secondary screening.

Similarly, if a suspicious item is detected by the AIT, the suspicious passenger is screened by a second officer with a wander while the following passenger continues through the AIT. The AIT station becomes available until after the security officer in charge of secondary body screening becomes available.

After the x-ray screening, cleared items enter a conveyor that delivers the items to the exit roller in the same order in which the items entered the x-ray. Passengers identify their items and stay around the exit roller until they have collected all their items. Up to six trays or carry-on items fit on the exit roller. If there is not a space available for the x-ray operator to continue delivering cleared trays, the operator stops the x-ray operation until a space opens for a tray to be delivered. Alarmed items, diverted to the manual diverter roller, are taken individually to a secondary screening station by a security officer. The security officer advises the passenger to collect the rest of his cleared items from the exit roller and follow him to the secondary screening station. The security officer waits for the passenger in the secondary screening station to ensure that the passenger can see what the officer is doing with the items.

We considered two performance measures to evaluate the performance of the models: the time to composure and the passenger throughput. The time to composure corresponds to the period from when passengers join the queue for checking their documents with a TDC officer up to the time when they are able to pick their items from the exit roller. The TSA has a standard limit of ten minutes for this measure. The passenger throughput corresponds to the average number of passengers screened by the AIT, if the system operates at full capacity.

Solution Prototype 1

The first solution prototype consists of replacing the exit roller of one of the two lanes for a continuously circulating conveyor where items circulate until they are collected by their respective passengers. Figure 2 displays how the layout in Figure 1 would change after this circulating conveyor is incorporated.

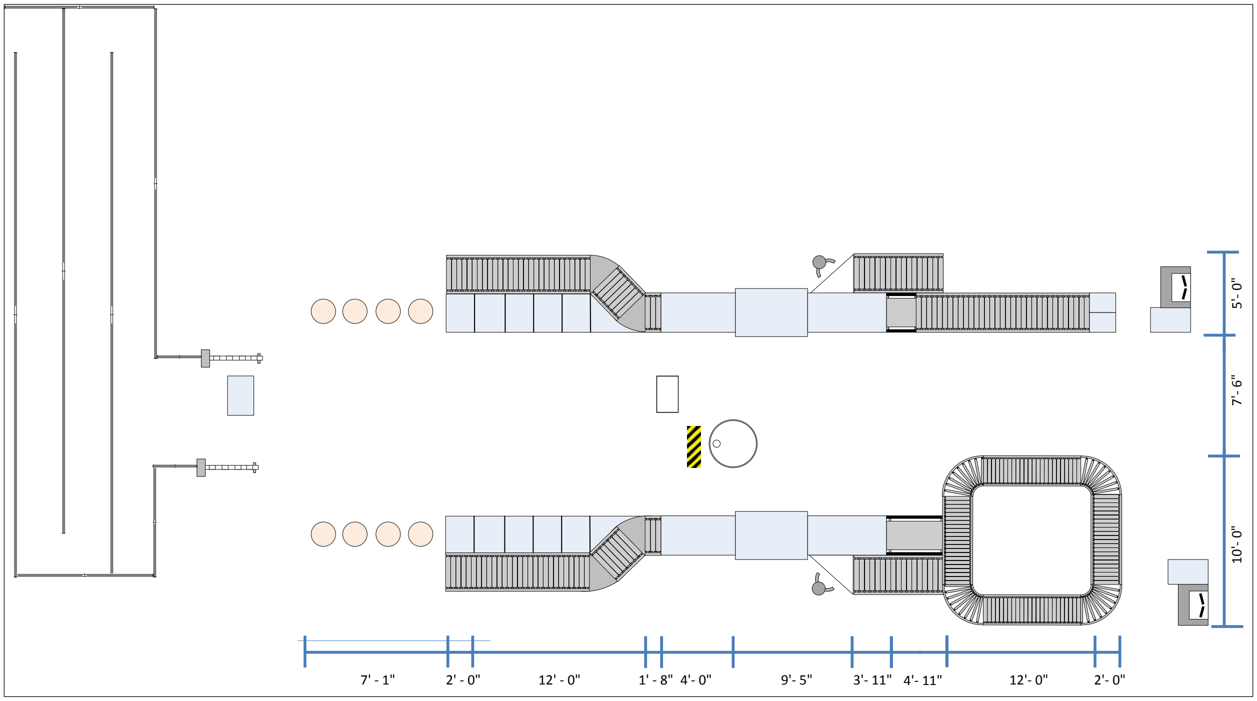

Figure 2. Solution Prototype 1 Layout

After the TDC process, passengers having a number of trays above a specific threshold to be determined by the experimental analysis are directed to the lane having the circulation conveyor in place. On the other hand, passengers requiring a number of trays below the threshold are directed to the lane having the least number of passengers waiting. In the case that both lanes are even in number of passengers waiting, priority will be given to the lane having the circulating conveyor.

At most six passengers can be waiting around the conveyor to collect comfortably their items. It was assumed that passengers avoid running after their items. Thus, upon having been cleared by the body screening process, passengers proceed to one of these six spaces to wait for their items. Items are delivered to the conveyor, where they circulate individually, each in one cell of the conveyor, checking for their passenger in each of the six conveyor spaces. If an item identifies a passenger with the same serial number, the item exits the conveyor, and it is put together with the other passenger's items. After the last item of the passenger exits the conveyor, the passenger releases the conveyor waiting space. We assume zero delay in unloading every item from the conveyor as items will continue circulating if they are not collected instantaneously.

Solution Prototype 2

The second solution prototype consists of implementing the circulating conveyor to both lanes. In this case, incoming passengers from the TDC station will be directed to the lane with the least number of passengers waiting. The purpose of this alternative is to show the gain in value (i.e. increase in throughput) when implementing the circulating conveyor in both lanes. Figure 3 displays a layout of this solution prototype.

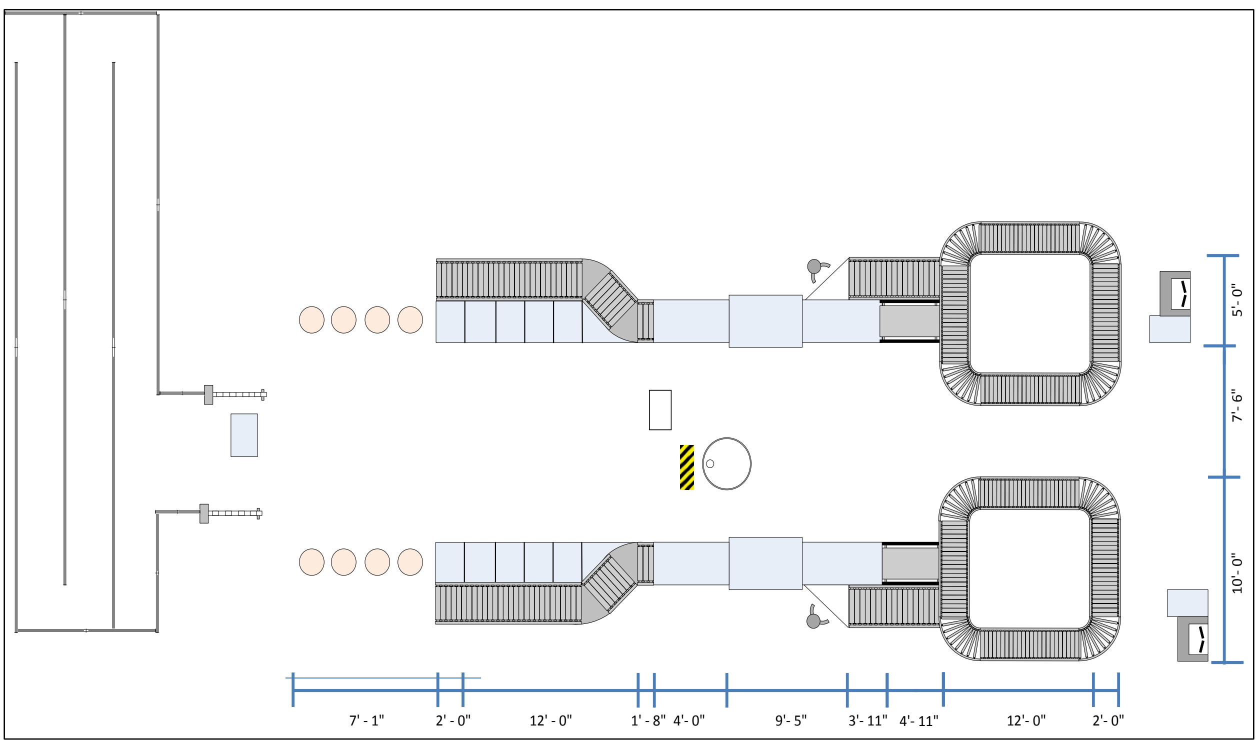

Figure 3. Solution Prototype 2 Layout

IV. MODELS' IMPLEMENTATION

Different from a spreadsheet or an analytical model, DES allows capturing the level of detail necessary for this type of analysis, where the system is subject to non-stationary arrival rates and variability in the service time parameters. In this section, we explore the key modelling issues to imitate the real system in a computer for the current configuration and the two solution prototypes. The Rockwell Software Arena environment, Version 15, was used for this purpose.

We identified four key modeling issues: the divestiture process for the three models; the composure process for the base model; the circulating exit conveyor for the two prototypes; and the secondary screening for the three models.

Divestiture Modeling

After passengers have been directed to one of the lanes, they proceed to one of the five-divestiture stations if there is one available, or wait in one of the four waiting spaces until one becomes available. Once in the divestiture station, the passenger entity loops according to the number of items he carries. In this loop, the model identifies whether each of his items is a carry-on or a tray item; and whether each item will pass the x-ray screening. We assume that if a passenger has any items, his last item will always be a carry-on item. The purpose of this loop is to ensure that the passenger keeps a record of the number of items he needs to collect at the exit roller, and the number of items that are going to be diverted to secondary screening. Exhibit 1 displays the pseudo-code for this logic.

Note in line 8, the variable *myXRayPT* corresponds to the preassigned x-ray processing time for the items' x-ray screening. If this random variable is greater than the threshold on the x-ray processing time limit, the item will be sent to secondary screening after the x-ray screening, and the variable storing the number of items to pick up from the exit roller is decreased by one. In Line 13, one item entity is created every time the passenger goes through the loop.

```
1 myCounter = 1
2 myCarry-On = TRUE
3 myNumItemsToPickUp = myNumItems
4 WHILE myCounter <= myNumItems
5    If (myCellIndex < myNumItems)
6        myCarry-On = FALSE
7    EndIf
8    If (myXRayPT > myXRayLimit)
9        mySecondaryScreening = TRUE
10       myNumItemsToPickUp = myNumItemsToPickUp -1
11   EndIf
12   myCounter = myCounter +1
13   SEPARATE 1 item from passenger
14 END WHILE
```

Exhibit 1. Separate Passengers from Items Logic

Upon having been created, the items queue to seize, one by one, the space where the passenger loads each item onto the conveyor. The passenger, on the other hand, waits in a hold construct until all of his items are on the divestiture conveyor. Subsequently, immediately after an item accesses the conveyor construct, it releases the loading space for the following item, and creates a logical entity that is placed in a batch along with the other logical entities of the same passenger. Once all of the passenger's logical entities have been grouped together, the collective entity signals the passenger with its identification number to release the passenger from the hold construct. Exhibit 2 displays the pseudo-code for this logic.

Items

```
SEIZE loading space
DELAY for loading
ACCESS divestiture
RELEASE loading space
SEPARATE dummy entities
CONVEY to x-ray
```

Item Dummy

```
BATCH myNumItems
SIGNAL Entity.SerialNumber
DISPOSE
```

Passenger

```
If (myNumItems > 0){
     WAIT for signal == Entity.SerialNumber
EndIf
GOTO AIT station
```

Exhibit 2.Divestiture Process Logic

Composure Modeling in the Current Configuration Model

The composure process of the current configuration was modeled using a signal-seize-hold-release logic. Essentially, we need to model how items roll over the exit roller after they are delivered from the downstream conveyor. Exhibit 3 displays the pseudocode for this logic. In Line 1, the item being delivered to the first space of the exit roller signals the item in the hold of the first space, so the item in the hold moves to the next space. Then, the signaling item seizes the first space in Line 2, and exits the composure conveyor in Line 3.

```
 1 SIGNAL item in Hold S1
 2 SEIZE Resource S1
 3 EXIT Composure Conveyor
 4 SEPARATE dummy item
 5 // send dummy to MATCH with passenger
 6 WHILE myCounter <= 4
 7         If(NQ(MEMBER(QueueSpacesSet, myCounter)) <= 0)
 8                 WAIT for signal(myCounter)
 9         End if
10         myCounter = myCounter + 1
11         SIGNAL item in HoldSpaceSet(myCounter)
12         SEIZE ResourceSpaceSet(myCounter)
13         RELEASE ResourceSpaceSet(myCounter - 1)
14 END WHILE
15 Infinite HOLD for S5
```

Exhibit 3. Logic for Item Rolling on Exit Roller

Next, in Line 7, the item in the first space checks whether there is another item coming immediately behind. If this is true, the item signals the item in front and seizes the following space. If no item is coming immediately behind, the item enters the hold construct of the first space, and waits for the signal of a rolling item or for the passenger to pick it up. This is the same for spaces 2 through 4. If an item rolls all the way until Space 5 of the exit roller, the item enters an infinite hold, where it waits until its passenger picks it up. See Line 15.

Exhibit 4 displays the logic used for modelling how passengers collect the rolling items from the exit roller. After items seize the first space of the roller, and exit the composure conveyor, they create a logical entity that is sent to match with the passenger (See line 4 in Exhibit 3). This logical entity acts like a messenger that notifies the passenger that one of his items is ready to be picked up. Once the passenger has been matched with one of his items' logical entities (See Line 7 in Exhibit 4), he proceeds to look for an item. He starts searching from Space 5 (i.e. the space farthest away from the x-ray). In this way, we ensure that he collects the item corresponding to the logical entity to which he was matched. For this reason, the attribute *myCounter* in Line 9 in *Exhibit 4* is initialized to 5, and is decreased by 1 as the passenger goes through the loop (i.e. moves closer to the x-ray while looking for his items).

The passenger may find his items in the queues of the space resources or in the queues of the hold constructs. If the passenger finds an item in one of the resource queues, the item releases the space corresponding to *myCounter* -1, because at the time, the item is physically in the previous space although it is in the process of seizing the space corresponding to *myCounter*. On the other hand, if the passenger finds an item in one of the hold queues, the item releases the space corresponding to *myCounter*, because the item is physically on the space corresponding to the loop counter.

```
1 If(myNumItems == 0)
2         DISPOSE passengers
3 Else
4         If(myNumToPickUp == 0)
5                 GOTO SecondaryScreening
6                Else
7                 A: MATCH with item dummy
8                 SearchID = Entity.SerialNumber
9                 myCounter = 5
10                B: SEARCH in QueueSpacesSet(myCounter)
11                If SearchID == Entity.SerialNumber
12                        REMOVE item from QueueSpacesSet(myCounter)
13                        // the removed entity makes the delay for unloading
14                        // and releases the previous space
15                        // if item is removed from the queue for S1, it exits the Composure
16                        MATCH with removed entity
17                        myNumItemsCollected = myNumItemsCollected + 1
18                Else
19                        SEARCH in HoldSpacesSet(myCounter)
20                        If SearhID == Entity.SerialNumber
21                                REMOVE item from HoldSpacesSet(myCounter)
22                                //The removed entity makes the delay for unloading
23                                //And it releases the current space
24                                MATCH with removed entity
25                                myNumItemsCollected = myNumItemsCollected + 1
26                        Else
27                                myCounter = myCounter - 1
28                                if myCounter <= 0
29                                        GOTO B
30                                End if
31                        End if
32                End if
33        End if
34 End if
35 If myNumItemsCollected >= myNumItemsCollected
36        If myNumItemsToPickUp == myNumItems
37                DISPOSE
38        Else
39                GOTO Secondary Screening
40        End if
41 Else
42        GOTO A
43 End if
```

Exhibit 4. Passenger Collecting Items Logic

After the passenger removes an item, he checks whether he needs to collect any other item from the roller. If this is true, he returns to the match construct to be matched with another logical entity of his items, and repeats the search process again. Otherwise, he checks whether there is any of his items at secondary screening. If this is true, he proceeds to secondary screening. Otherwise, he leaves the checkpoint.

Composure Modeling of the Circulating Conveyor

The composure process for the prototype models follows a different logic than in the current configuration for the lanes where the exit roller is replaced for a continuously circulating conveyor. Exhibit 5 displays the logic that passengers follow in a circulating conveyor lane.

```
If(myNumItems == 0)
    DISPOSE passengers
Else
    If(myNumToPickUp == 0)
        GOTO SecondaryScreening
    Else
        SEIZE space around conveyor from ResourceSet (Save mySetIndex)
        DELAY walk time to Space
        HOLD in Space at HoldSet (mySetIndex)
    End if
End if
```

Exhibit 5. Passenger Logic for Composure in a Circulating Conveyor Lane

After the passenger finds he needs to pick up some items from the circulating conveyor, he seizes the closest space available around the conveyor. He delays some random time for walking to the space, and enters a hold construct linked to the space that he seized.

On the other hand, items are delivered to the circulating conveyor by the composure conveyor. Upon accessing the circulating conveyor, they exit the composure conveyor and convey by sequence from space 1 to space 6 of the conveyor. In each space, items get assigned an index associated with the space on which they are. They search the passenger in the hold queue of the space associated with their index. If they find a passenger with the same serial number in a particular space, they exit the conveyor and get batched with the other items of the passenger. If items do not find their passenger, they continue circulating to the next station. When they reach station 6, but they have not found their passenger, their attribute *Entity.JobStep* is reset to 0, so they can recirculate again from station 1. Line 20 in Exhibit 6 displays this part of the logic.

```
1 ACCESS circulating conveyor
2 EXIT Composure Conveyor
3 CONVEY by sequence to Station in Station Set
4         Space 1.Station
5         Space 2.Station
6         Space 3.Station
7         Space 4.Station
8         Space 5.Station
9         Space 6.Station
10 A: (For every Station) ASSIGN mySetIndex
11 vSN = Entity.SerialNumber
12 J = 0
13 SEARCH Passenger
14        MEMBER(Holds Set, mySetIndex)
15        Starting Index: 1
16        Ending Index: NQ(MEMBER(Holds Set, mySetIndex)
17        Search: vSN == Entity.SerialNumber
18        if (j == 0)
19             if (Entity.Job.Step == 6)
20                  ASSIGN Entity.JobStep = 0
21             End if
22             CONVEY by sequence
23             Goto A
24        Else
25             EXIT circulating conveyor
26             BATCH by Entity.SerialNumber (Batch Size: myNumCells)
27             REMOVE passenger from HOLD Set (MEMBER(Holds Set, mySetIndex)
28             DISPOSE Extra entity
29             RELEASE Space around Conveyor
30             If myNumItemsToPickUp == myNumItems
31                DISPOSE
32             Else
33                GOTO Secondary Screening
34             End if
35        End if
```

Exhibit 6. Item Logic for Composure in a Circulating Conveyor Lane

Secondary Screening

Similar to divestiture, secondary screening is the same for the three models. Upon the items get conveyed out from the x-ray through the downstream roller, they are directed to either the composure conveyor or the diverter roller if they require secondary screening. The diverter roller is inclined, so items roll to the end of the roller with the force of gravity. Thus, the diverter roller was also modelled using a conveyor construct. Exhibit 7 displays the logic that items follow on the diverter roller.

```
If (mySecondaryScreening == FALSE)
        GOTO composure
Else
        ACCESS diverter roller
        RELEASE downstream roller
        CONVEY to the end of diverter roller
        BATCH items of passenger temporarily (Entity.SerialNumber)
        SEIZE 2Screening Officer
        SEPARATE temporary batch
        SEPARATE one dummy per item
```

Exhibit 7. Item Logic on Diverter Roller

Upon accessing the diverter roller, items exit the downstream roller. Next, they convey to the end of the roller, and items of a single passenger are grouped together as a representative entity of the items. This entity seizes the secondary security officer. Next, the representative entity is separated again into individual items, and each item creates a duplicate of its own. The duplicates proceed to a match construct while the actual items are grouped again into a representative entity. This entity is a representation of the officer itself, who goes back and forth between the diverter roller and the secondary screening station to bring the items of the passenger to the secondary screening station. Thus, in the diverter roller, this officer entity is matched with one of the duplicates (See Line 3 in left hand side of Exhibit 8), so the duplicate exits the conveyor while the officer entity walks to the secondary screening station. This logic was necessary to ensure items would only exit the diverter roller after the officer picked them up to take them to secondary screening. The officer entity goes back to the diverter roller and repeats the process until he has taken all the items of the passenger to the secondary screening station. After all of the items have been taken, the officer is released, so he can take serve other passengers.

Items

```
1 BATCH items again into representative item entity
2 myCounter = 1
3 A: MATCH  with one item dummy
4 ROUTE to secondary screening
5 myCounter = myCounter + 1
6 if(myCounter < myNumItems - myNumItemsToPickUp)
7     ROUTE back to diverter roller
8     GOTO A
9 Else
10     RELEASE 2ScreeningOfficer
11     MATCH item representative entity with
12     passenger //to wait for the passenger to
13     //start secondary screening
14     SEIZE 2ScreeningOfficer
15     DELAY representative entity for secondary screening
16     SEPARATE items from officer entity
17     //Dispose items
18     DELAY walking back to diverter roller
19     RELEASE 2ScreeningOfficer
20     DISPOSE
21 End if
```

Item Dummies

```
1 Item dummies
2 MATCH with representative entity of items
3 EXIT diverter roller
4 DISPOSE
```

Exhibit 8. Item Logic on Diverter Roller

Next, at the secondary screening station, the items' representative entity is matched with the passenger, so secondary screening is only performed when the passenger is present (See Line 10 in left hand side of Exhibit 8). After the secondary screening takes place in Line 12, the officer entity creates duplicates based on the passenger's number of items in secondary screening. These items are disposed while the officer entity walks back to the diverter roller and releases the officer resource in Line 19.

V. MODEL ESTIMATION OF PARAMETERS

We faced several difficulties in obtaining permission from the TSA to collect the data for the distribution parameters of our models. Therefore, we obtained these parameters from the literature, providing details on their collected observations. Given the difficulties associated with physically collecting data from real security checkpoints, we dedicated this section to compile some the efforts found in the literature related to data collection and estimation of the most commonly used parameters in the simulation modeling of security checkpoints to facilitate the simulation modeling and validation for future studies on security checkpoints.

Data Collection on Arrival Patterns

De Barros and Tomber (2007) assert that passenger arrivals to the checkpoint depend on the flight schedule and the passenger earliness of arrival (EOA) profiles. They claim, a common simplifying assumption is to use the same EOA regardless of the time of the day although variation does occur during the day. Passengers flying in the morning tend to arrive much closer to the departing time than those flying at noon or in the afternoon. They do obtain different EOA profiles for domestic and international travelers. After extensive collection of data a Seattle-Tacoma International Airport, they obtained the EOA profiles displayed in Table 1. They combine these EOA with the airport flight schedule to obtain an arrival schedule for passengers and luggage' screening.

Table 1.Earliness of Arrival Profile at Seattle-Tacoma International Airport

Time to Departure	*Interval*	*Domestic*	*International*
0-15	1	0%	0%
15-30	2	2%	0%
30-45	3	2%	1%
45-60	4	6%	4%
60-75	5	13%	13%
80-90	6	22%	21%
90-105	7	24%	23%
105-120	8	19%	19%
120-135	9	10%	11%
135-150	10	2%	5%
150-165	11	0%	2%
165-180	12	0%	1%
180-195	13	0%	0%
195-210	14	0%	0%
210-225	15	0%	0%
225-240	16	0%	0%

In addition, Paul et al. (2009) studied the factors that may affect the passenger flow patterns. Using an analysis of variance (ANOVA) of a general linear model, they concluded that both day and time of the day and the interaction between both have a significant effect on the passenger volume. Figure 4 displays the total passenger volume per day of the week. In addition, their ANOVA results suggested that four different patterns should be used to generate the passenger arrivals of a week. These are Monday, Saturday, Sunday and Tuesday through Friday. Figure 5 displays the variation of the passenger volume throughout the day for each four-day pattern.

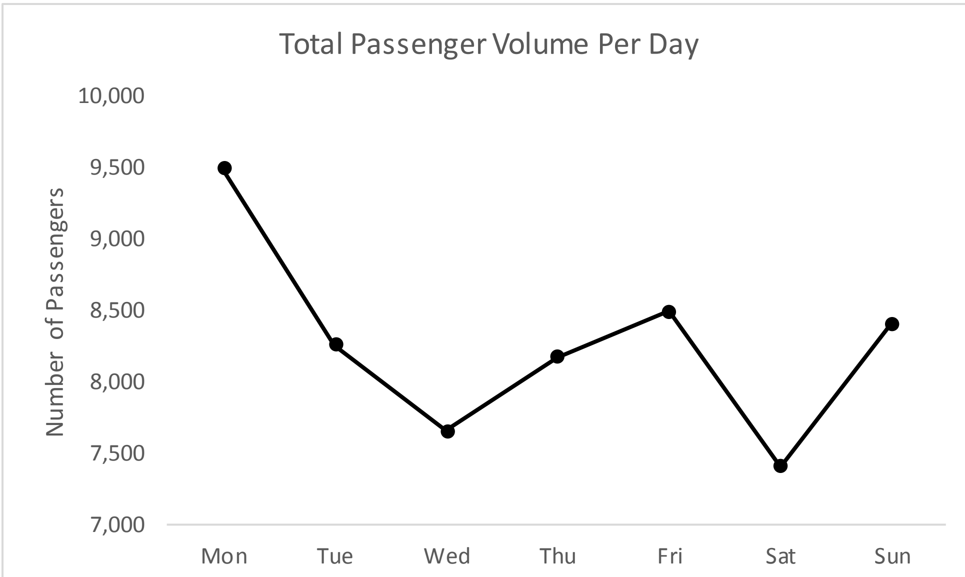

Figure 4. Passenger Volume per day of the week

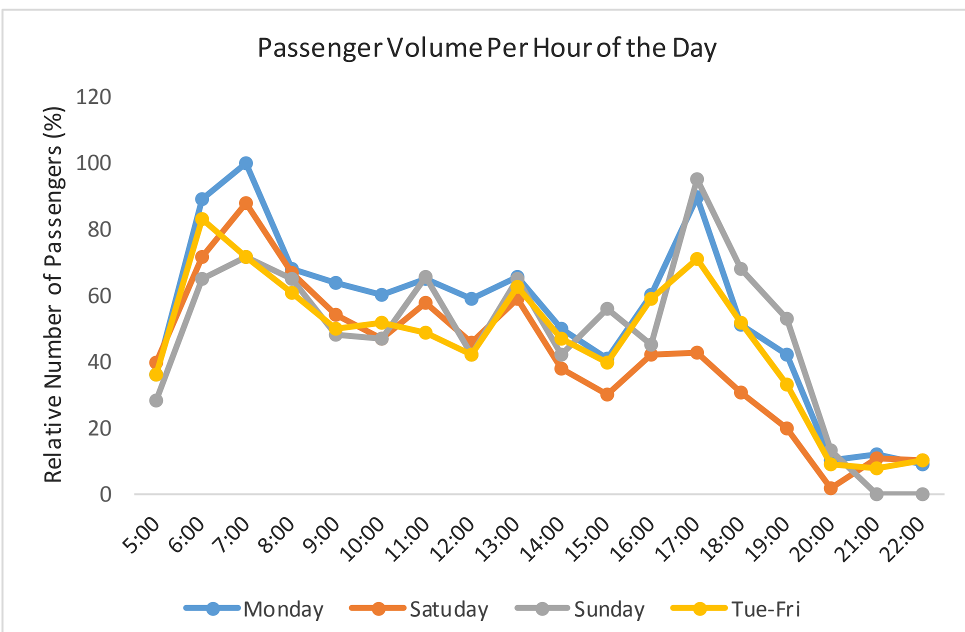

Figure 5. Passenger Volume per hour of the day

As Paul et al. (2009) suggest, the highest levels of passenger traffic occur between 5 am and 8 am, and between 4 pm to 6 pm. In addition, Mondays displayed the highest passenger traffic volumes while Saturdays displayed the lowest. Nonetheless, the authors failed to specify the size of the airport from which they collected these passenger traffic volumes.

Nie et al. (2011) used the observations provided by Paul el al. (2009) in Figure *5* to obtain the arrival schedule in Table 2. It displays the average number of arrivals by day and time period.

Table 2. Arrival Schedule from 5:00 am to 11:00 pm

Time period	Mon	Tue–Fri	Sat	Sun
5:00–6:00	432	432	480	336
6:00–7:00	1068	996	876	780
7:00–8:00	1200	864	1056	864
8:00–9:00	792	732	792	780
9:00–10:00	768	600	648	576
10:00–11:00	720	612	552	564
11:00–12:00	768	588	696	792
12:00–13:00	696	504	552	492
13:00–14:00	780	768	708	756
14:00–15:00	600	564	456	504
15:00–16:00	492	480	372	660
16:00–17:00	720	708	516	540
17:00–18:00	1092	864	528	1128
18:00–19:00	624	624	384	816
19:00–20:00	528	396	240	648
20:00–21:00	120	108	48	168
21:00–22:00	144	96	132	0
22:00–23:00	108	120	120	0

Paul et al. (2009) also provide their observations on the number of lanes open per day and per hour of the day. Their statistical tests showed that the number of lanes open does not vary significantly according to the day of the week, but it does vary according to the hour of the day. *Figure 6* displays the upper and lower bounds on the number of lanes open for both normal and selectee lanes. However, the authors failed to specify whether the number of normal lanes included the pre-check lane.

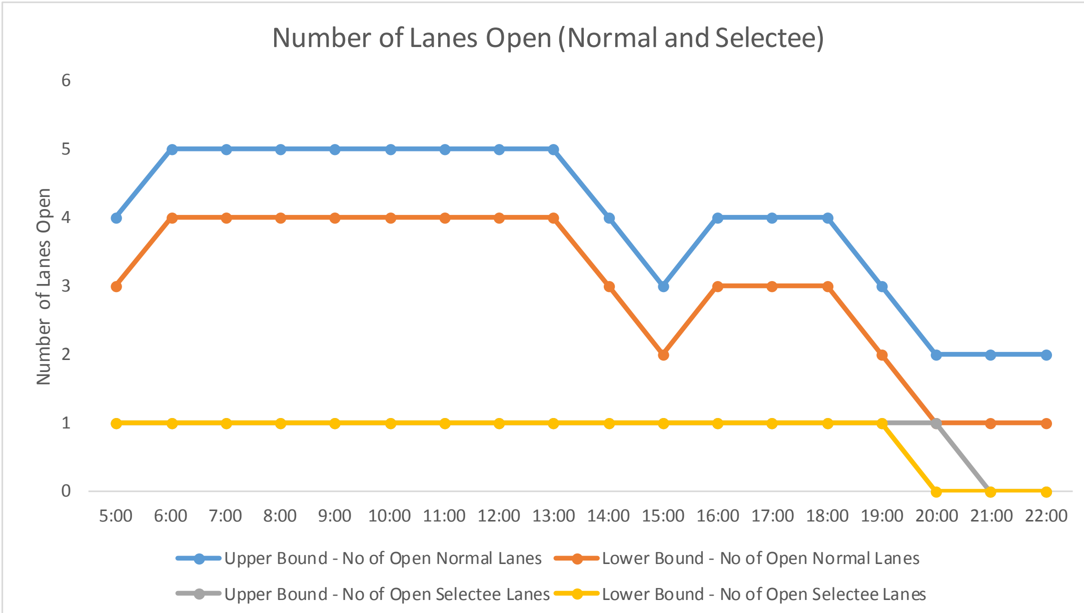

Figure 6. Number of Lanes Open per Hour of the Day

De Lange, Samoilovich and Der Rhee also provide their arrival patterns along with the average number of lanes open for each hour the day. They collected these observations at a large airport in Western Europe. Figure *7* displays the graph summarizing their observations.

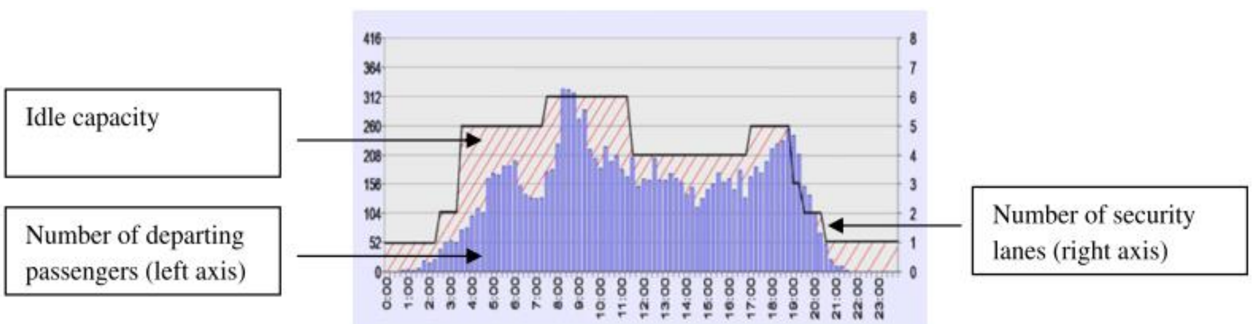

Figure 7. Arrival Patterns and Lane Idle Capoacity at a Larger Airport in Western Europe

The distribution for the walking velocity of the passengers and the security officers was also obtained from literature. We used a triangular distribution with parameters 2.93, 4.4 and 5.86 feet per second (Hobbs, Rossetti and Faas, 2006).

Data Collection on Inspection Times at the X-Ray and Secondary Screening

Leone and Liu (2011) provide the distributions for the processing times at the x-ray and the secondary screening. They obtained this information from the TSA, who provided data on over 500 screened passengers. They assert the secondary screening follows a uniform distribution between two and five minutes. In addition, they provide the distribution of the x-ray screening time versus the number of cleared and not cleared items from the x-ray screening. Figure 8 displays a graph summarizing their observations. We fitted a distribution to these observations and obtained a gamma distribution with a shape parameter equal to 3.49 and a scale parameter equal to 2.05. Both parameters were obtained from observations given in seconds.

Leone and Liu (2011) also claim that the percentage of cleared items during the x-ray inspection ranges from 89% to 97%. Therefore, the probability that an item requires secondary screening ranges between 3% and 11%.

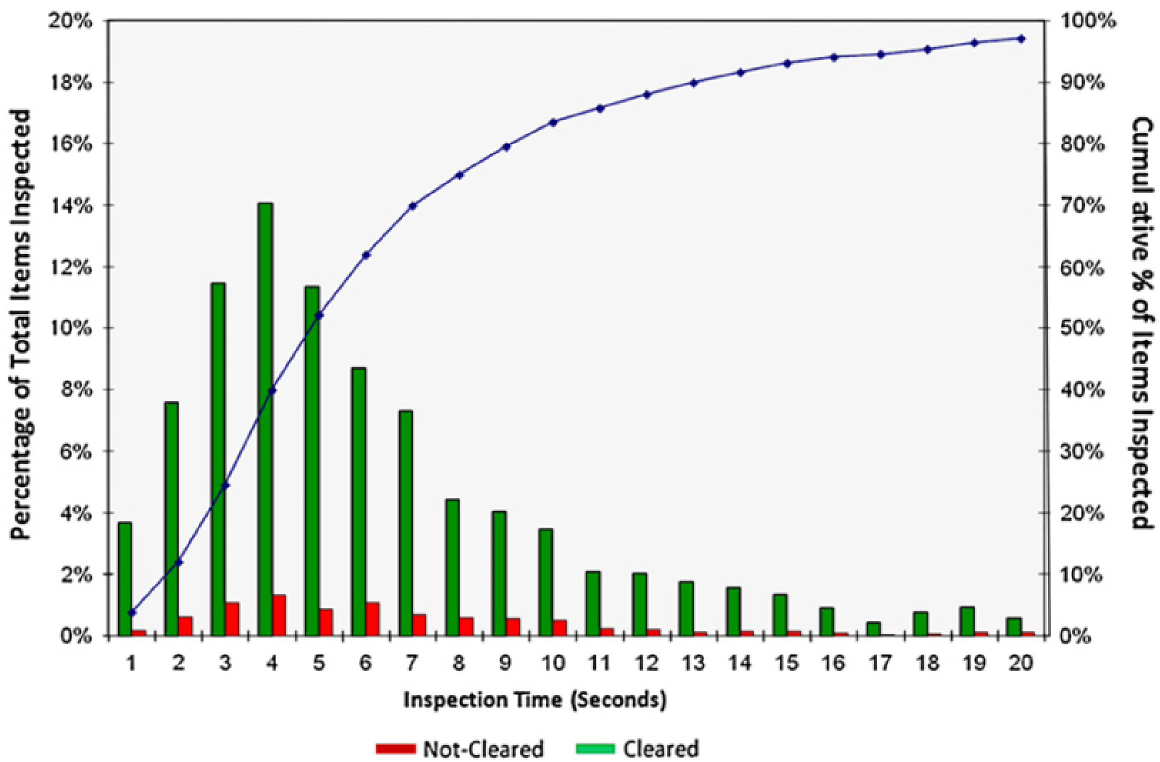

Figure 8. X-Ray Screening Inspection Times

Nie et al. (2011) also provide details on their distributions for the x-ray and secondary screening inspections. They use a triangular distribution with parameters 10, 12 and 14 seconds for the x-ray inspection of a selectee lane, and parameters of 8, 10, and 12 seconds for the x-ray inspection of a non-selectee lane. For the manual inspection at secondary screening, they fit a gamma distribution with shape parameter of 2 minutes and scale parameter of 2.05 minutes.

For our models, we used the gamma distribution we obtained from Leone and Liu's observations for the x-ray inspection. In addition, we used Nie et al.'s gamma distribution on the inspection time for secondary screening, because it allowed using the coefficient of variation to try different levels of the mean for the experimentation section.

Data Collection on Passengers' System Times and Throughput

In supporting the validation for their simulation models, Paul et al. provide the data they collected on the passengers' system time for the four days for which they identified a unique arrival pattern. Figure 9, Figure 10, Figure 11, and Figure 12 display, respectively, their observations for each of the four arrival patterns. Each plot contains three data series, displaying the average, maximum and minimum system times for each hour of the day from 5 am to 11 pm.

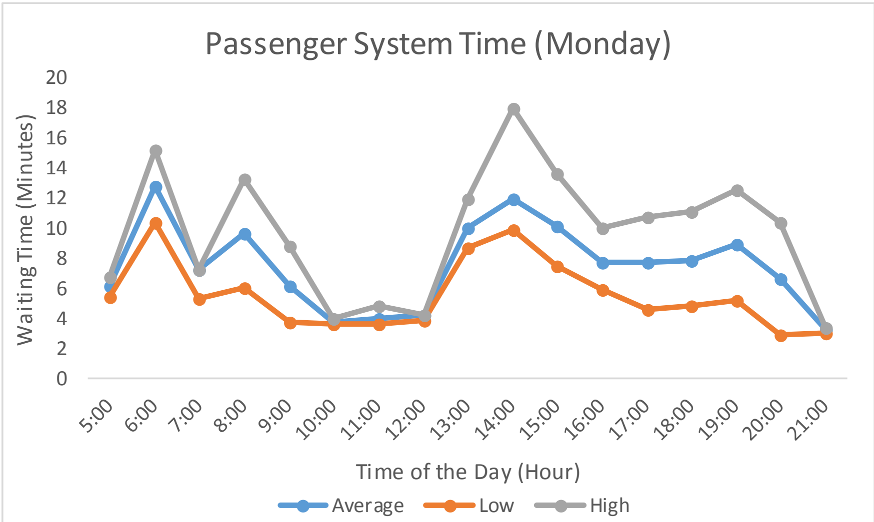

Figure 9. System Time of Passengers on Monday

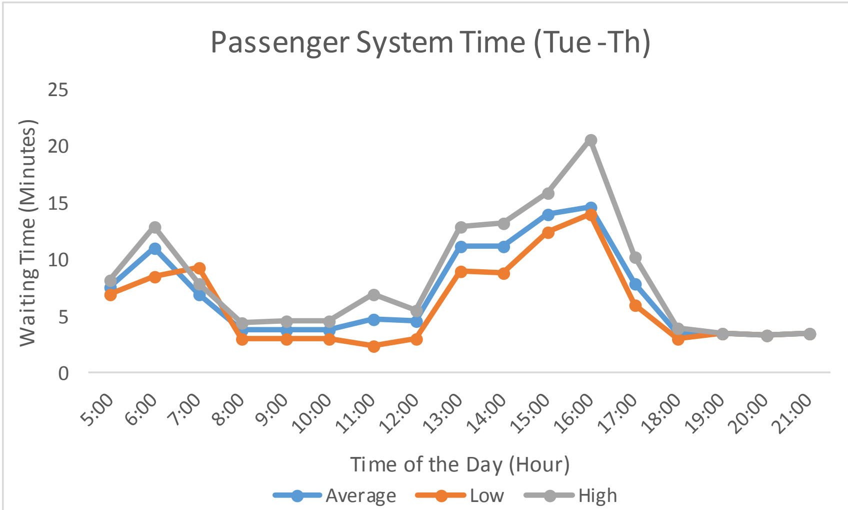

Figure 10. System Time of Passengers from Tuesday to Thursday

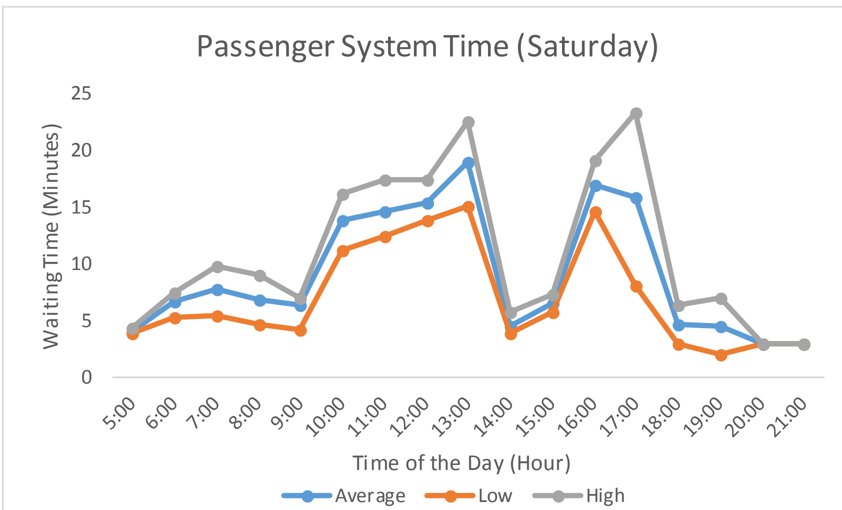

Figure 11. System Time of Passengers on Saturday

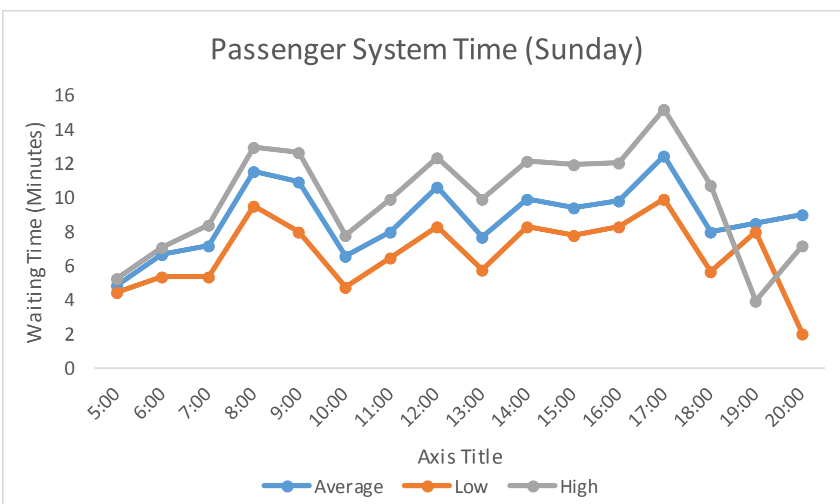

Figure 12. System Time of Passenger on Sunday

Wetter, Lipphardt and Hofer (2010) collected eighteen measurements on the average throughput and the number of passengers requiring secondary screening inspection in a medium-size airport in Zurich. All measurements were obtained during peak hours. Figure 13 displays the plot where they summarized their collected data.

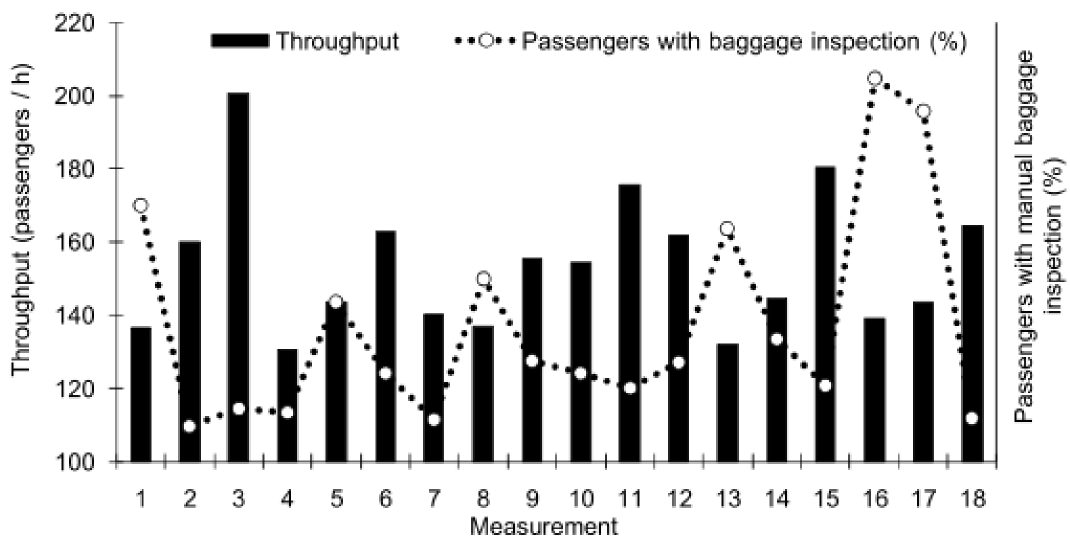

Figure 13. Throughput and relative number of passengers with manual baggage inspection

Data Collection on the Distribution for the Number of Items per Passenger

Paul et al. (2009) also provided details on the distribution for the number of items per passenger. They observed passengers requiring more trays during high-passenger traffic hours, specifically mornings of weekdays when most passengers are business passengers. Thus, the distribution of the number of items per passenger looks left-skewed for high-passenger-volume hours, symmetrical for medium-passenger-volume hours and right-skewed for low-passenger volume hours. Table *3* Table *1*displays the three discrete distribution they obtained from their analysis. These three distributions were used in the models of our study to generate the number of items per passenger.

Table 3. Distribution of Items per Passenger (Paul et al, 2009)

	Items per Passenger					
Passenger Volume	*0 Items*	*1 Item*	*2 Items*	*3 Items*	*4 Items*	*5 Items*
High	0	5	10	20	40	25
Medium	2.5	10	20	40	20	7.5
Low	2.5	25	35	20	12.5	5

Dorton and Liu (2016) also provide details on their distribution for the number of items per passenger. Different from Paul et al. (2009), they only provide a single discrete distribution for a general traffic volume of passengers, and they adjust their distribution such as every passenger has at least one item. Table *4* displays the probability mass function for the distribution they used in their simulation model.

Table 4. Distribution of Items per Passenger (Dorton and Liu, 2016)

	Items per Passenger				
# of Items	1	2	3	4	5
PMF	0.03	0.36	0.44	0.16	0.01

Four our models, we used the distributions from Paul et. al, because their parameters are specific for the traffic volume of passengers.

VI. MODELS' VALIDATION AND VERIFICATION

The model verification consisted of ensuring that the key modeling issues worked exactly as intended. We accomplished this by carefully animating the key modeling issues in the three models while debugging what looked unusual in the animation. Figure 14, **Error! Reference source not found.**, and Figure 16 display a picture for the base configuration and the two solution prototypes.

The models' validation consisted of making sure that the model accurately represented the real system. According to Leone and Liu's airport classification, the volume of passengers taken into account for this study corresponds to the volume of a medium hub airport where passenger arrival volumes for peak hours reach 200 passengers per hour for a two-lane system. According to their literature review, waiting times at medium hub airports are slightly below the TSA standard 10 minute limit, and the AIT runs at a capacity of 150 passengers per hour (Leone and Liu 2011).

Using an arrival rate of 200 passengers per hour, a threshold of 11 seconds for the x-ray processing time, as suggested by Leone and Liu's study, we obtained an average AIT throughput of 165.71 passengers per hour with a half width of 25.40 passengers based on a 95% confidence interval. In addition, we obtained an average waiting time of 3.56 minutes with a half width of 0.34 minutes. In addition, an average 91% of the passengers with a 0.02 half-width have a waiting time under 10 minutes. Note that our system seems to have slightly better performance measures than the system studied by Leone and Liu, because our system accounts for the new automated divestiture system implemented at ATL in 2016. This system is expected to reduce waiting times by 30% (Solomon 2016).

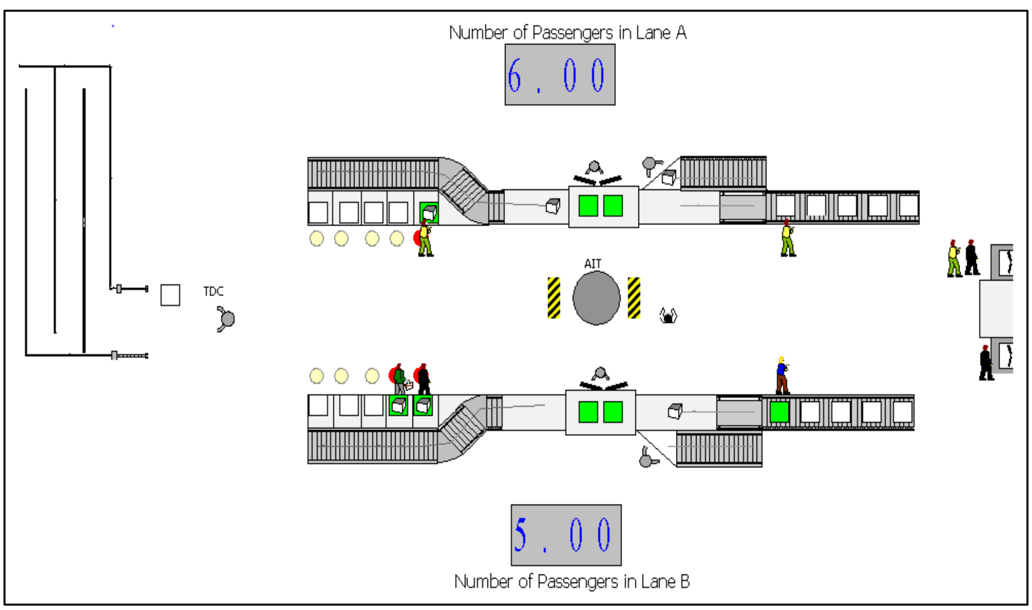

Figure 14. Animation of Base Configuration Model

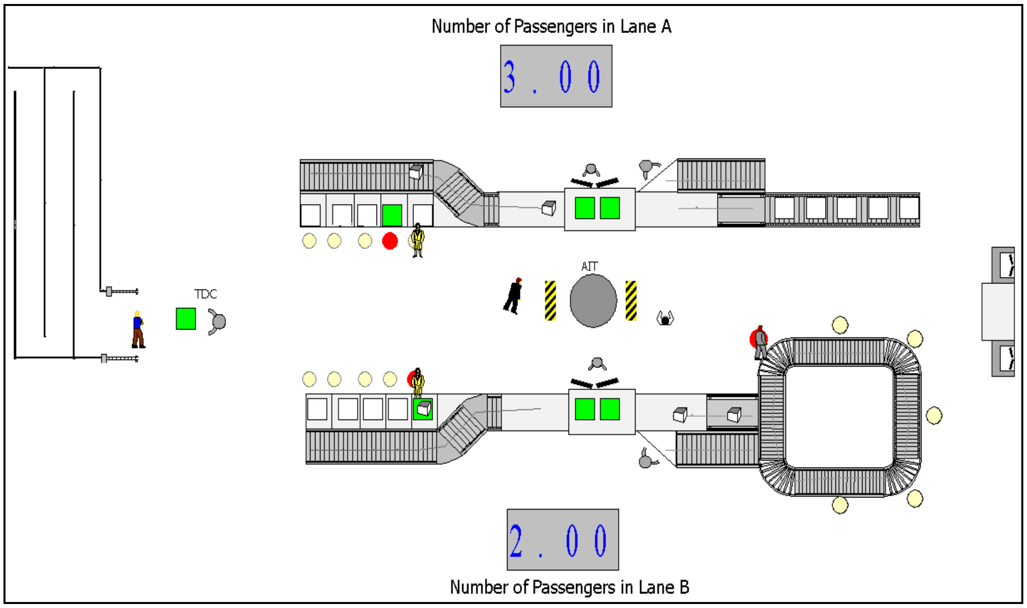

Figure 15. Animation of the Prototype 1 Model

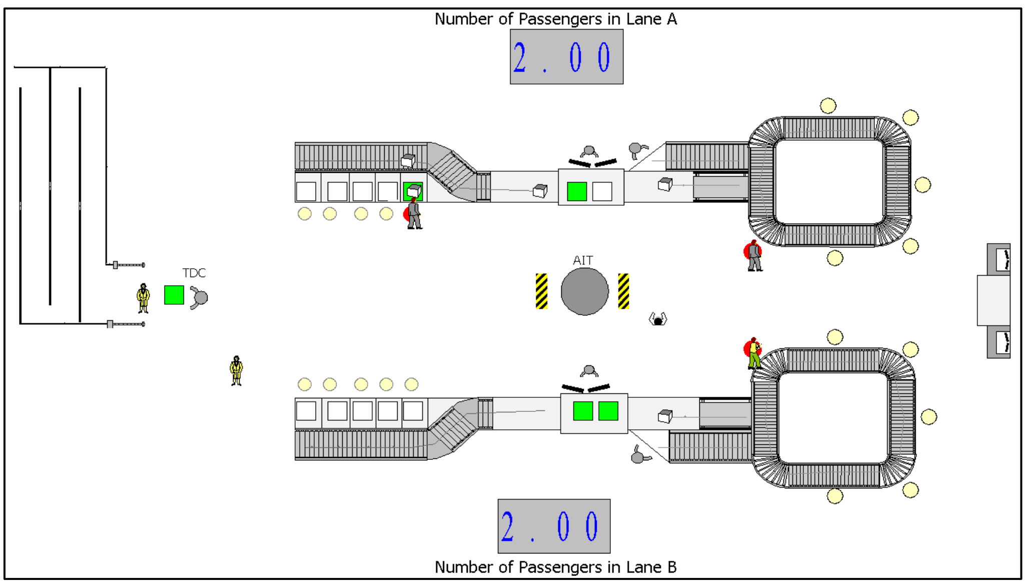

Figure 16. Animation of Second Prototype Model

VII. EXPERIMENTATION AND RESULTS

The performance of the circulating conveyor highly depends on the amount of items being delivered to the conveyor. If the flow level of items being delivered from the x-ray station is low, the circulating conveyor could be unnecessary. In addition, as Leone and Liu (2011) concluded in their study, limiting the x-ray processing time of every item while routing to secondary screening any item requiring additional screening time, could significantly reduce the waiting time of passengers. Moreover, the circulating conveyor is expected to accelerate the item flow by providing more space and clearing the roller's space faster. Thus, the first stage of the experimentation consisted of investigating the effect of the circulating conveyor on the optimal x-ray processing time limit, proposed by Leone and Liu's study. First, we verified Leone and Liu's findings using the simulation model for the base configuration. Then, we observed how the threshold changed with the models for the first and second prototypes. Additional sensitivity analysis was performed using the coefficient of variation of the secondary screening distribution.

In addition, given that a lane having the circulating conveyor is expected to process passengers faster than a lane featuring a traditional exit roller, using the model for the first prototype, we explored the possibility of directing passengers likely to take longer, to the lane best suited for their processing. Because passengers who carry more items may require additional time for processing, we expect the passenger's processing time to be positively correlated with the quantity of items carried by the passengers. Consequently, we used simulation optimization to find the threshold on the maximum number of items that a passenger can have to be able to process at the lane featuring a traditional layout. Passengers carrying a number of items above this threshold will be directed to the lane featuring the circulating conveyor in order to compensate for the additional time that these passengers take.

Lastly, we explored the possibility of replacing two traditional lanes with one circulating conveyor lane. We conduct a sensitivity analysis on the arrival rate of passengers in order to determine the arrival rates under which the performance of one circulating conveyor lane is comparable to the performance of a traditional two-lane system. In the following sections, we will examine each part of the experimentation in detail.

Threshold on the X-Ray Processing Time Limit

This portion of the experimentation consisted of finding the x-ray processing time limit that results in the minimum average system time, using the simulation model for the base configuration as well as the models for the first and second prototypes.

Leone and Liu (2011) performed their experiments on a system operating at capacity. According to their proposal, their system was unable to complete the processing of all the 200 incoming passengers without their suggested recommendation. Consequently, we performed this stage of the experimentation with a system at capacity. As we observed during the validation section, our models, featuring the new divestiture system, were able to process 200 pph, completely with 90% of the passengers being processed within 10 minutes. Therefore, we decided to increment the mean arrival rate of the exponential distribution of our models to 300 pph for this stage of the experimentation in order to have a system operating at capacity.

First, an exploratory analysis was performed to investigate the relationship between the x-ray processing time limit and the system time in the base model. Next, a polynomial regression analysis was conducted to find the limit resulting in the minimum system time. Lastly, a sensitivity analysis was performed by varying the parameters of the secondary screening distribution, and testing how the optimum limit would change with the prototype models.

Exploratory Analysis

For an initial screening of the two variables, 176 scenarios of 15 replications each were performed, using the model for the base configuration. Each scenario differed in the x-ray processing time limit parameter, which ranged between 7.5 and 25 seconds among the 176 scenarios. Figure *17* displays the results for this initial screening.

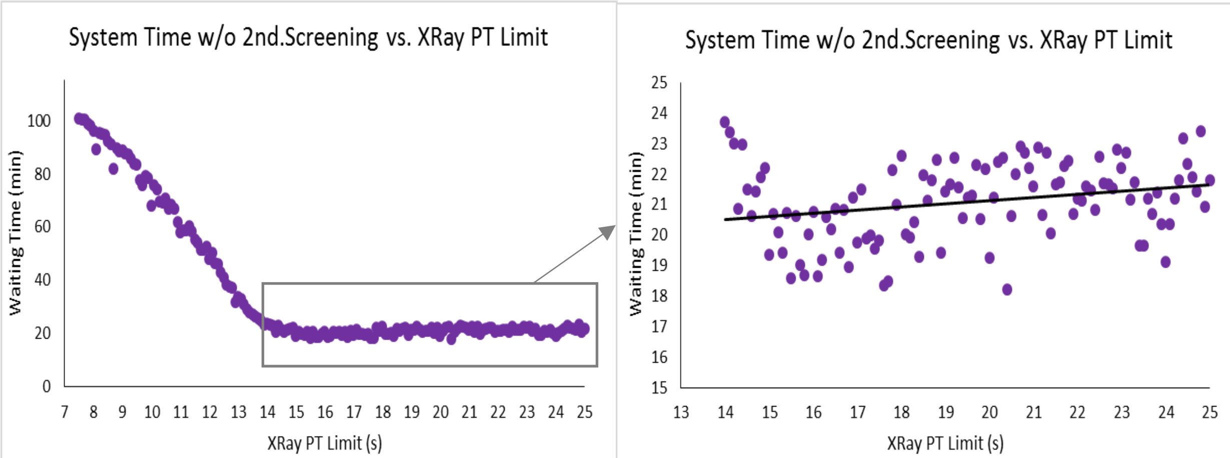

Figure 17. Response to Change in the X-Ray Processing Time Limit (Base Model)

As we can observe in the picture to the left, the metric decreases almost linearly as the limit increases to 15 seconds. In other words, limits under 15 seconds cause the system to direct a large proportion of items to secondary screening, because there is little tolerance in the time that an item can spend at the x-ray screening. This increases the probability that the diverter roller becomes full, because many items are being directed to secondary screening. As a result, an incoming item, attempting to access the diverter roller, remains in the downstream roller until there is space in the diverter roller. Consequently, the lane backs up all the way to the TDC, which significantly increases the system time of passengers awaiting in the lines.

Figure 18 displays how the probability that the diverter roller in a lane is full decreases as the x-ray processing time limits increases to around 15 seconds. With limits above 15 seconds, the probability that the diverter roller becomes full is very small.

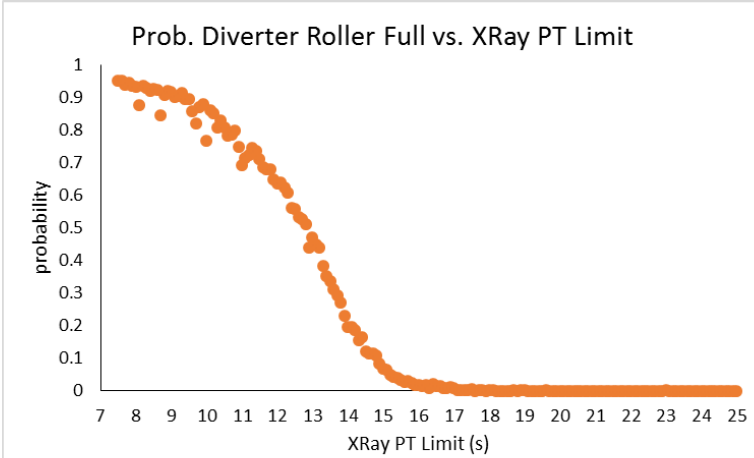

Figure 18. Probability that the Diverter Roller is full

In addition, we observed a slight increase in the response variable with limits above 17 seconds. The picture to the right in Figure 17 displays the trendline associated with this slight increase. An analysis of variance was performed on limits above 15 seconds to determine whether the x-ray processing time limit had any effect on the system time with limits above 15 seconds. Levels of 15, 30 and 45 seconds were used as the levels for this analysis. For each level, eight observations were obtained. Table *5* displays the experimental design with the 24 observations.

Table 5. Experiment Design for ANOVA on X-Ray PT Limit.

X-Ray PT Limit	System Time (min)			
	19.951	19.736	19.118	19.963
15	19.915	21.204	20.344	20.925
	23.323	23.342	20.497	22.506
30	20.924	22.026	23.872	23.035
	21.941	24.395	20.487	22.392
45	21.362	22.499	24.067	22.848

From the analysis of variance, we obtained that the effect of the x-ray processing time limit on the system time is significant with limits above 15 seconds (p-value = 0.0). See Figure 40 in the Appendix for additional details on this analysis of variance. We assumed equal variance among the replicates of each factor level. In addition, the analysis of residuals in Figure 19 shows that the residuals are independent and normally distributed.

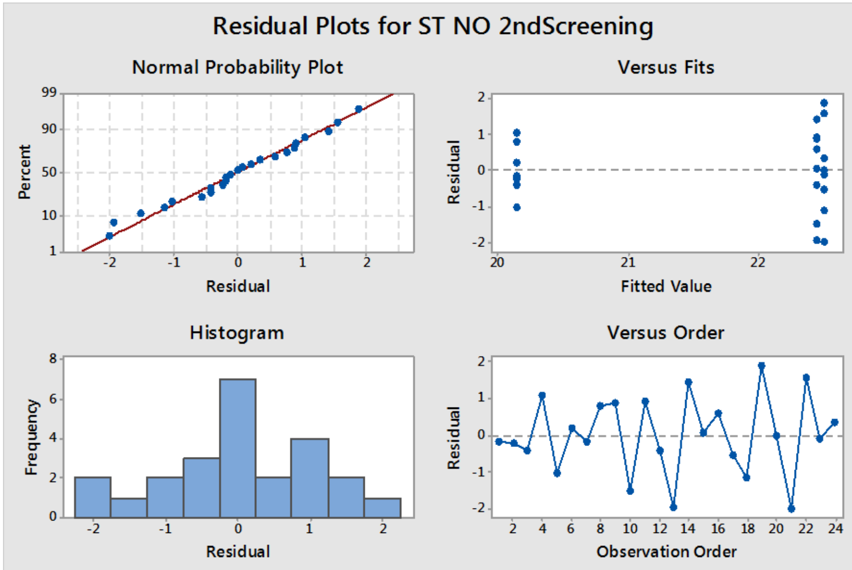

Figure 19. Residuals Analysis on System Time vs. X-ray PT Limit (Base Model and CV = 0.71)

Using a Tukey's test, we conducted a multiple comparison on the three factor levels to verify the significance of the mean difference between each possible pair of x-ray limit. Figure 20 displays the confidence intervals for these multiple comparisons.

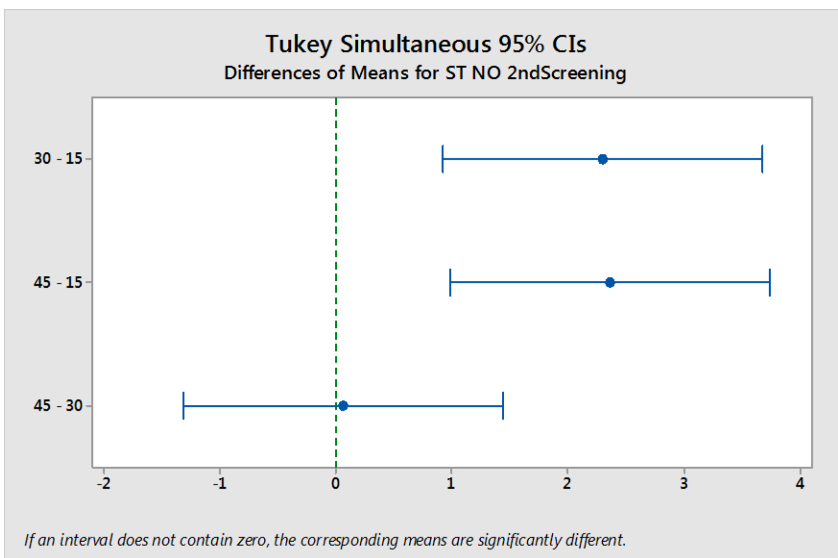

Figure 20. Multiple Comparisons on System Time vs. X-ray PT Limit (Base Model CV = 0.71)

As we can see, the mean difference in system time is significant between the 15-second limit and the 30-second limit, and between the 15-second and the 45-second limit. In both combinations, a limit of 15 seconds results in a shorter mean system time than limits of 30 and 45 seconds. This evidence supports Leone and Liu's suggestion of imposing a limit on the x-ray processing time, because there is a penalty on imposing a large x-ray processing time limit. On the other hand, the mean difference is not significant between the 30-second limit and the 45-second limit. This was expected, because the chance that an item requires an x-ray processing time of 45 seconds is very small given the distribution of the x-ray processing time. As a result, setting the limit at 45 seconds has almost the same effect as setting the limit at 35 seconds, because about the same proportion of items would be directed to secondary screening in either case.

Polynomial Regression Analysis

A polynomial regression analysis was used to determine the x-ray processing time limit resulting in the minimum system time. The total time up to the end of the composure process, before the secondary screening process, was used as the response variable while the x-ray processing time limit was used as the predictor variable. We excluded the secondary screening processing time from the response metric to avoid the secondary screening time overshadowing the change in the processing time of the other components in the system. Varying the x-ray processing time limit may have a significant effect on the system time of those passengers whose items require secondary screening. However, this effect is not necessarily proportional to x-ray limit's effect on the other components of the system. Additional metrics that were observed through the process include statistics associated with the secondary screening process such as processing time in this area, the number of passengers waiting to be served at secondary screening and the probability that the diverter roller in a lane is full.

A linear model of the order k was fitted to the response obtained from varying the predictor variable in Figure *17*. The polynomial regression model obtained was of the form

$$y = \beta_0 + \beta_1 x + \beta_2 x^2 + \beta_k x^k + \epsilon \quad (1)$$

Where y is the response variable, β_0 is the intercept term, x is the predictor variable, k is the polynomial order satisfying a coefficient of determination above 95%.

Next, the minimum was found by obtaining the critical points of the polynomial function over the range of the x-ray processing time limits of interest such as

$$f'(x) = 0 \qquad for \qquad 7.5 \leq x \leq 25 \tag{2}$$

The critical points provide the x-ray processing time limits where the slope of the function's tangent line is equal to zero. The optimal limit is the critical point resulting in the minimum system time from using the polynomial regression model.

Figure 21 displays the polynomial regression line that was fitted to the curve in Figure 17.

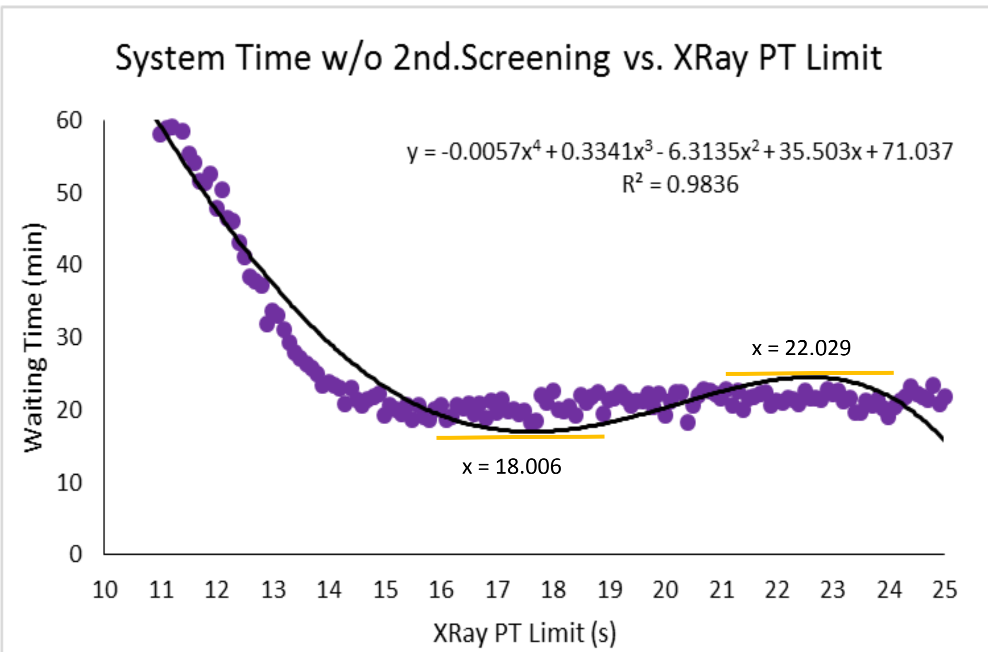

Figure 21. Polynomial Regression on Base Model (CV = 0.71)

The limits identified around the curve are the two critical points over the range from 7.5 and 25 seconds. As we can observe from the curve, the critical point resulting in a minimum system time of 14.625 minutes is the limit of 18.006 seconds. Additional details on the significance of the regression are provided in Table 6.

Table 6. ANOVA and Regression Statistics

	df	*SS*	*MS*	*F*	*Significance F*
Regression	4	112,628.23	28,157.06	2,570.22	0
Residual	171	1,873.32	10.96		
Total	175	114,501.55			

	Coefficients	*Standard Error*	*t Stat*	*P-value*
Intercept	71.037	30.168	2.355	0.020
X Variable 1	35.503	8.402	4.225	0.000
X Variable 2	-6.313	0.838	-7.537	0.000
X Variable 3	0.334	0.036	9.387	0.000
X Variable 4	-0.006	0.001	-10.389	0.000

<u>Sensitivity Analysis on the Coefficient of Variation of the Secondary Screening Parameters</u>

A limit on the x-ray processing time of 18 seconds increases the risk of possible threats as opposed to a limit of 11 seconds. With a limit of 18 seconds, fewer items are being directed to secondary screening, because there is a high tolerance in the time that the x-ray operator can spend screening an item. As a result, there is a smaller chance of detecting a true threat, because the item may only be screened by the x-ray operator. On the other hand, a limit of 11 seconds increases the chance that an item is directed to secondary screening, but it requires additional resources in secondary screening, so secondary screening does not become a bottleneck.

The mean time of the secondary screening processing time distribution could be reduced by improving the process at secondary screening or adding additional resources. Thus, the coefficient of variation of the secondary screening distribution parameters was used to determine whether reducing the mean of the secondary screening distribution could reduce the risk associated with possible threats. The distribution was modelled using the gamma distribution, because of the large variance associated with secondary screening process.

The coefficient of variation is the proportion of the mean that corresponds to the standard deviation of the distribution for the secondary screening processing time. Equation 3 displays a mathematical form of this definition, where *CV* represents the coefficient of variation, μ is the mean of the processing time distribution, and σ is the standard deviation. A lower mean increases the coefficient of variation, assuming the variance of the distribution is kept constant.

$$CV = \frac{\sigma}{\mu} \tag{3}$$

We developed three additional response curves, differing in the coefficient of variation of the parameters for the secondary screening processing time. Figure *22*, Figure *23* and Figure *24* display these curves. Similar to the response curve in Figure *17*, these curves were developed from 176 scenarios, differing in the x-ray processing time limit.

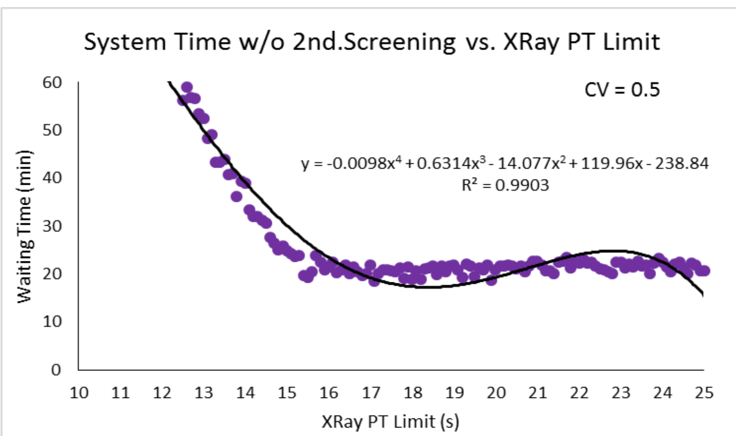

CP (s)	*System Time (min)* *__Predicted__*
19.0239	12.229
21.9785	14.451

Figure 22. Response Curve on Base Model (CV = 0.5)

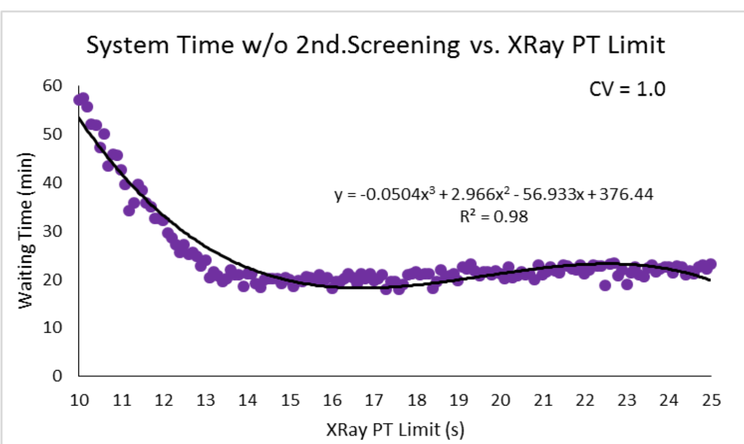

CP (s)	*System Time (min)* *__Predicted__*
16.742	18.110
22.491	22.898

Figure 23. Response Curve on Base Model (CV = 1.0)

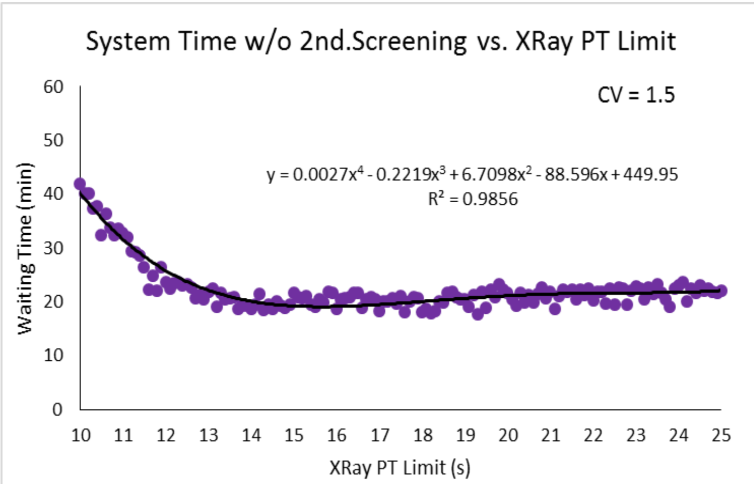

CP (s)	*System Time (min) Predicted*
16.1673	18.162
19.6513	18.764

Figure 24. Response Curve on Base Model (CV = 1.5)

A polynomial regression model was fitted to each of the three response curves. Details on the statistical significance of the three regressions were provided in the Appendix section in Table *7*, Table *8*, and Table *9*, respectively. The tables to the right of each graph display the critical points (CPs) in the curves and the predicted system times obtained from the regression models. The highlighted fields in each table correspond to the critical points resulting in the minimum system time in each curve according to the predicted values. From looking at these results, it seems that the critical point associated with the minimum system time decreases as the coefficient of variation increases. In other words, reducing the mean of the secondary screening distribution by adding newer technology or making the process more efficient reduces the x-ray processing time limit resulting in the minimum system. As a result, the risk associated with possible threats also decreases, because a lower limit increases the probability that an item requires secondary screening. Future work on this study should include a statistical analysis that the optimum limit decreases as the mean of the secondary screening distribution decreases, using response curves. Cahya, Del Castillo and Petersons (2004) present a methodology for computing confidence intervals on the optimal factor levels obtained from optimizing a general response surface model.

Wan et al. (2015) expands this approach to compute a confidence interval for a maximum point of a univariate polynomial function in a given interval.

An additional analysis of variance was made to determine whether the coefficient of variation of the parameters for the secondary screening distribution had any effect on the passenger system time when the x-ray limit was set at the optimum level. In other words, for this analysis, we tested statistically whether the coefficient of variation shifted the curves vertically in any direction. Using the base model, we obtained the average system time from 35 replications for each of the three pairs of coefficient of variation and optimum limit shown in Figure *22*, Figure *23*, and Figure *24*. This resulted in 105 observations of the system time. Similar to the previous analysis, the response variable for the system time did not include the secondary screening processing time. The analysis of variance showed that the coefficient of variation does not have a significant effect on the system time when running the model under the optimum x-ray processing time limit for each coefficient of variation (p-value = 0.74). Figure 42 in the Appendix provides the details on this analysis of variance. Figure 25 displays the confidence intervals on the mean difference for the three possible pair combinations.

As we can see, the three confidence interval on the mean differences overlap, meaning that the system times are statistically the same for the three coefficient of variation levels. Therefore, reducing the mean of the secondary screening distribution does not have an effect on the system time when setting the x-ray processing time limit at the optimal level. The analysis of residuals in Figure *26* shows that residuals are independent and normally distributed.

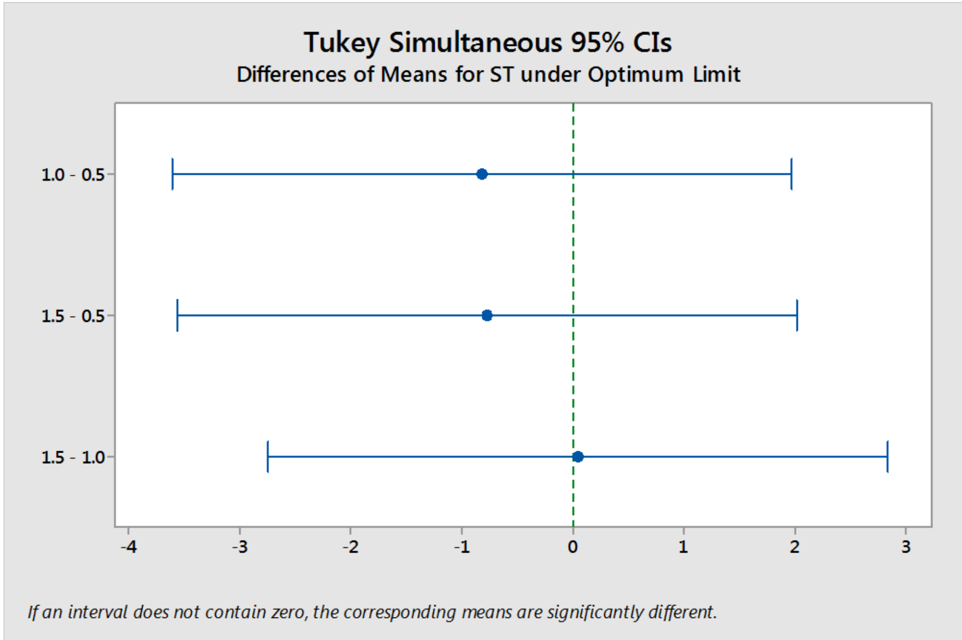

Figure 25. Multiple Comparison on System Time vs. Coefficient of Variation (Base Model and Optimum X-Ray PT Limit)

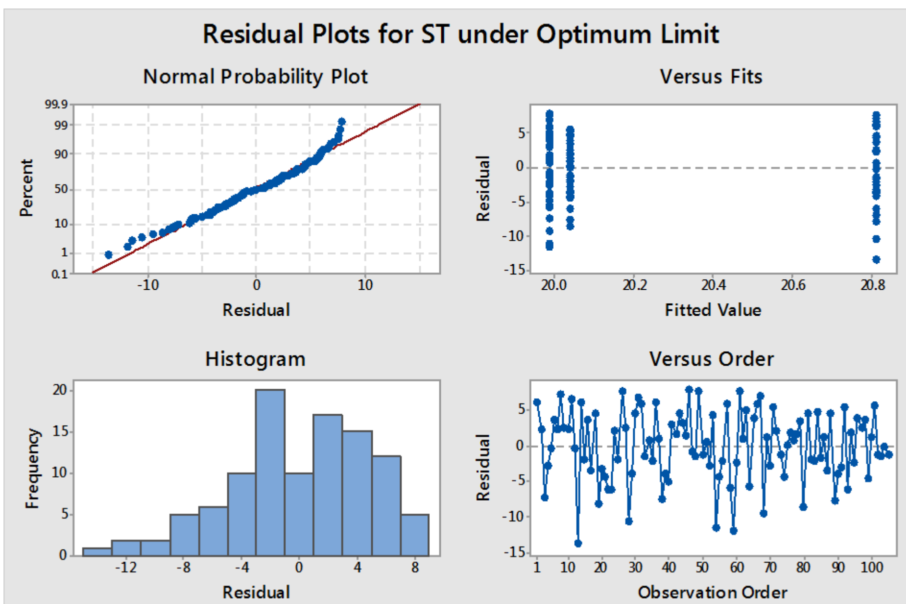

Figure 26. Residuals Analysis on System Time vs. Coefficient of Variation (Base Model and Optimum X-Ray PT Limit)

<u>Senitivity Analysis with First and Second Prototypes</u>

The second sensitivity analysis consisted of examining how the optimum limit for the x-ray processing time would differ for the first and second prototypes. Figure 27 displays the response curve for the first prototype, using a coefficient of variation of 0.71. It also displays the 4th-order polynomical regression model that was fitted to the curve. Figure 28 displays the response curve and regression model for the second prototype. The tables to the right of both graphs display the crirtical points, and the optimum limits for the x-ray processing time, highlighted in yellow. Details on the regression fit of the curves are provided in the Appendix in Table 10 for the first prototype's model and in Table 11 for the second prototype's model.

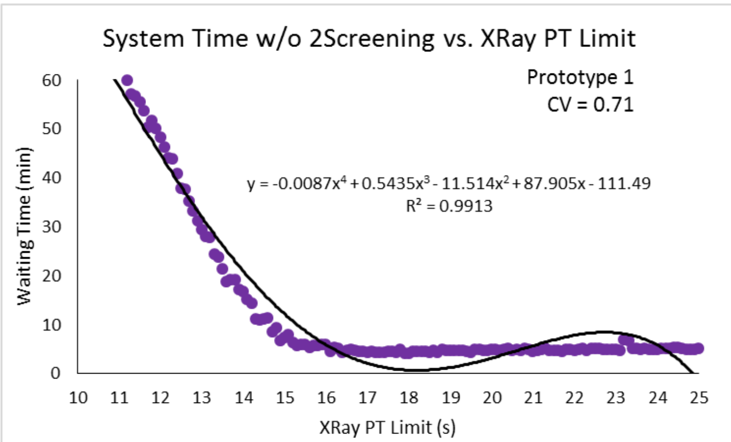

CP (s)	*System Time (min) Predicted*
18.7799	-3.808
21.9441	-1.192

Figure 27. Response Curve for Prototype 1 Model (CV = 0.71)

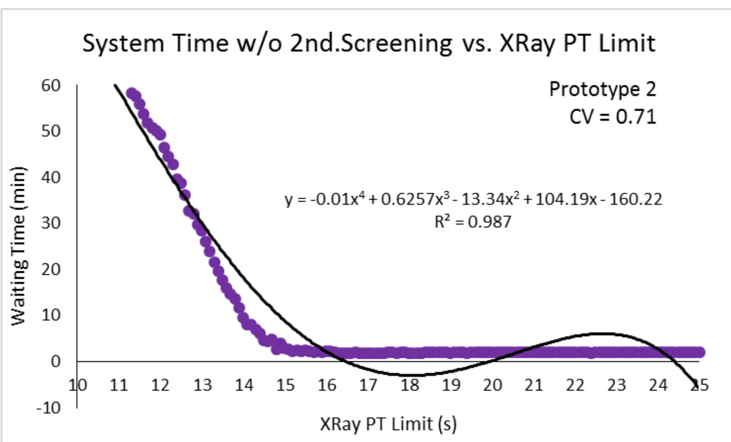

CP (s)	*System Time (min) Predicted*
18.6313	-7.987
21.9175	-4.699

Figure 28. Response Curve for Prototype 2 Model (CV = 0.71)

The shapes of both response curves are very similar to the response curve of the base model in Figure 17. The critical points resulting in the minimum system time in both regression models are very close to the optimum limit for the x-ray processing time in the base model as well. See

Figure 17. Future work should also include the statistical analysis on the effect of the proptotypes on the optimum limits for the x-ray processing time.

Nonetheless, the minimum system time for the first prototype seems to be lower than that of the base model. Moreover, the second prototype seems to have the shortest system time under the optimum limit. Statistical analysis was conducted on this hypothesis using an analysis of variance to test the significance of the models' effect on the system time of passengers under the optimum x-ray processing time limit. Similar to previous analyses, the system time response did not include the secondary screening processing time. We obtained the average system time of 35 replications for each of the three models under their respective optimum limits on the x-ray processing time. A coefficient of varaition of 0.71 was used in the three models. The analysis of variance showed that there is statistically significant difference among the system time of the three models (p-value = 0.0). Figure 43 in the Appendix displays the details on this analysis of variance. In addition, the analysis of residuals in Figure 29 shows that the residuals are independent and normally distributed.

A multiple comparison test was performed on the difference in system time means of the three models to determine which of the means differed among each other. The confidence intervals of the Tuckey's Test, in Figure 30, display the outcome of this analysis.

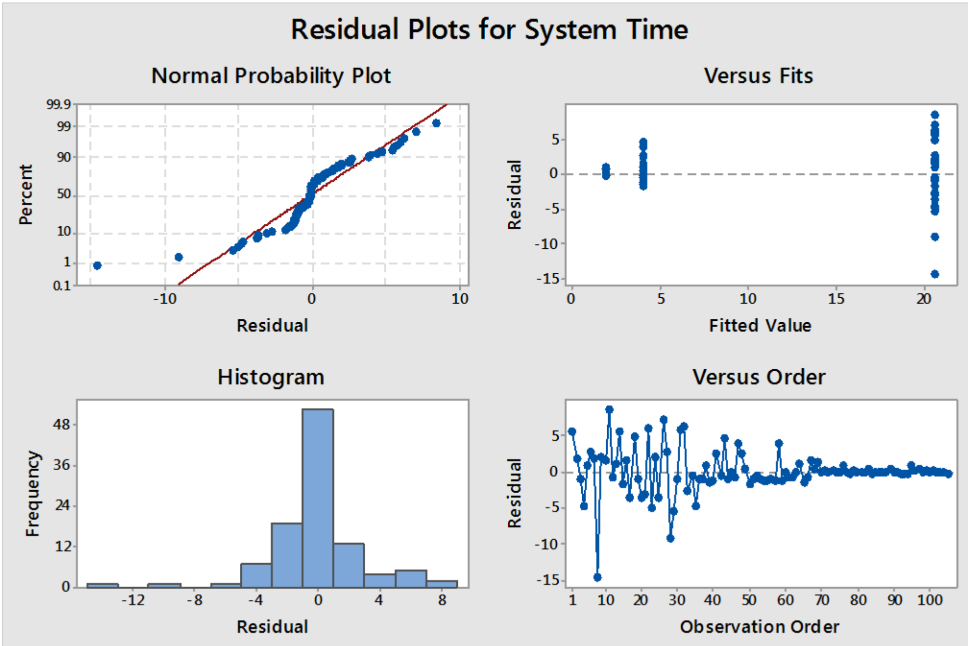

Figure 29. Residuals Analysis on System Time vs. Models
(CV = 0.71 and Optimum X-Ray PT Limit)

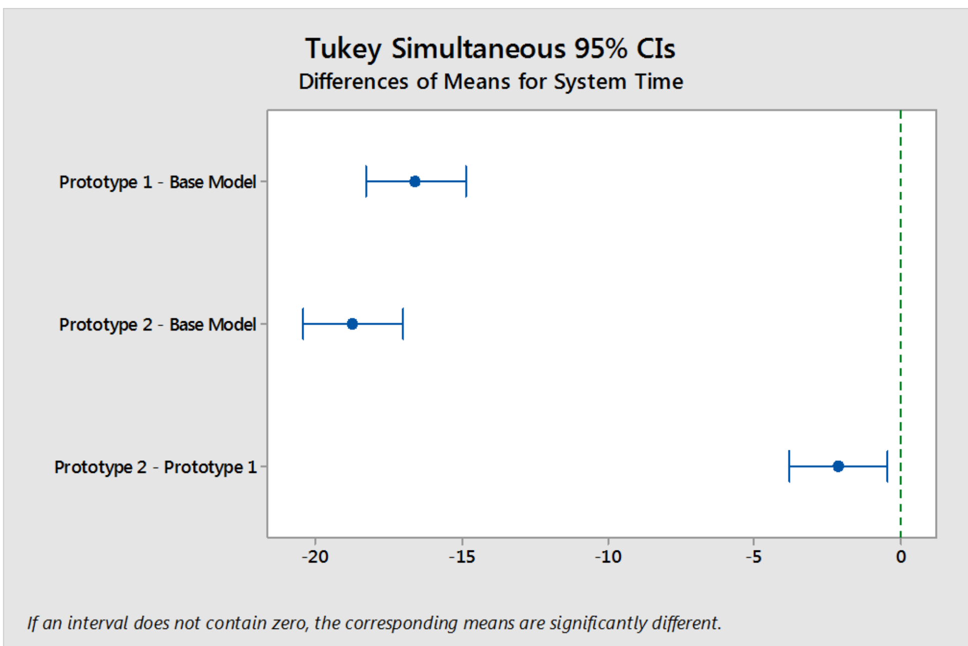

Figure 30. Multiple Comparison on System Time vs. Models
(CV = 0.71 and Optimum X-Ray PT Limit)

As we can see, the mean differences of the pairs do not overlap in any of the three confidence intervals. In other words, the mean differences are statistically significant for the three possible pairs. The mean system time of the base model under the optimum limit is significantly longer than those of the first and second prototypes. Thus, both prototypes have a statistically better performance than the base model in terms of system time. Similarly, the mean system time of the first prototype is significantly longer than the mean system time of the second prototype. In other words, the second prototype has statistically the best performance of the three models in terms of mean system time. This was expected, because the second prototype features the circulating conveyor in both lanes. However, the mean difference between the prototypes' system times is smaller than the mean difference between the system times for the first prototype and the base model. In other words, the mean system time reduction is much more significant from the base model to the first prototype, than from the first prototype to the second prototype. Therefore, the next section explores in more detail the first prototype, as it showed very promising results, and it requires less capital investment than the second prototype.

Threshold on the Number of Items per Passenger

In the three simulation models used for the previous section, passengers were directed to one of the two lanes, based on the number of passengers in the divestiture area. The directing officer would send passengers to the lane having the least number of passengers. Nonetheless, for the first prototype, the lanes differed in that, one lane featured a traditional exit roller while the other featured the circulating conveyor.

In addition, as we were able to see in the previous section, the circulating conveyor significantly reduces the processing time of passengers. In other words, the processing rate is lower for the lane featuring the circulating conveyor. In addition, passengers carrying more items are naturally expected to have a longer system time than those having fewer items. As a result, processing passengers with a large amount of items in the circulating conveyor lane may reduce the overall system time for the first prototype further, because the faster processing rate of the circulating conveyor may compensate for the longer time that these passengers take.

The purpose of this section consists of evaluating statistically the performance of a different rule for directing passengers to the lanes in the first prototype. Upon the TDC process, the directing officer will send passengers, having a number of items below a specific threshold, to the lane having the least number of passengers in the divestiture area, as in the original model. On the other hand, passengers having a number of items equal or greater than the threshold will follow this logic: if there is space for them to wait in one of the four waiting spaces before the divestiture stations of the circulating conveyor lane, they will be directed to this lane. Otherwise, the directing officer will send them to the lane having the least number of passengers in the divestiture area.

As we explained previously in Section 5, the discrete distribution for the number of items that the passengers carry was obtained from Paul et al. (2009). They provide three different distributions: one for high-traffic volume of passengers, one for medium-traffic volume, and a third for low-traffic volume. The high-traffic volume distribution ranges between 1 and 5 items while the other two range between 0 and 5 items.

For this part of the experimentation, we used the three distributions. As in any of the three cases passengers may have 1 to 5 items or 0 items, we varied the threshold on the number of items between 1 and 6 items among 180 runs of 2 replications each, for each distribution. We did not use zero as a threshold, because the system time of a passenger with zero items would be the same regardless of the lane he uses. Additionally, we used the threshold of six items to include the current scenario where passengers are directed based on the lane having the least number of passengers. Therefore, each threshold level had 30 replicates of the same experiment.

A separate analysis of variance was conducted for each of the three distributions, testing the effect of the number of items' threshold on the total system time. Different from the previous experimentation section, the response for the system time includes the processing at secondary screening. In addition, for this section, we are more interested in the results from simultaneously comparing the mean difference on the system time of all the 15 possible pair combinations among the six possible thresholds. Figure 31 displays the interval plot of the system time for the six thresholds, using the high-traffic volume distribution. As we can see, the scenarios with thresholds of four, five and six items seem to have the shortest mean system time. However, the threshold resulting in the minimum system time seems to be five items.

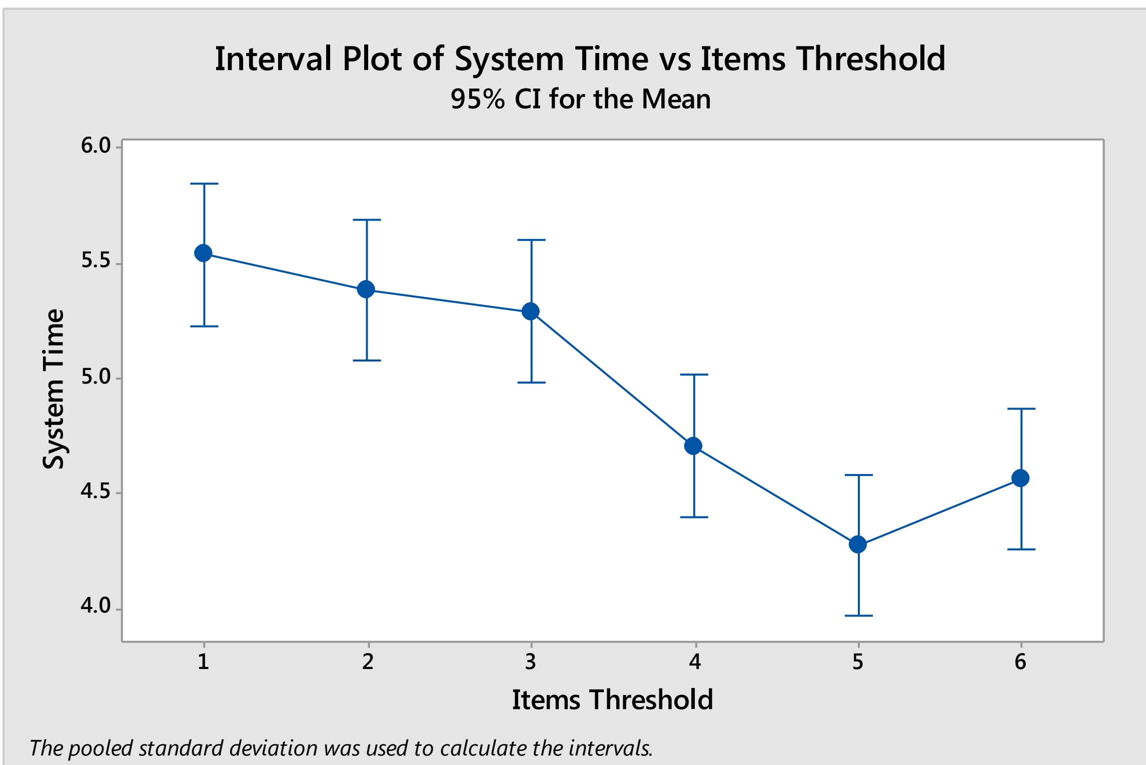

Figure 31. Interval Plot on System Time vs. Num. of Items Threshold
(High-Traffic Volume Distribution)

Figure 32 displays the results from simultaneously comparing the mean system time of the six scenarios. Similar to what we observed in Figure *31*, the lowest mean corresponds to the five items' threshold. However, the mean system times for the scenarios with thresholds of four and six items are statistically the same. The scenarios with thresholds of one, two and three items have statistically different mean system times. However, these system times are inferior to the system time of the current configuration. Therefore, for the high-traffic volume distribution, setting a threshold on the number of items to direct passengers to the circulating conveyor lane, does not make a significant difference in the mean system time of passengers.

Tukey Pairwise Comparisons

Grouping Information Using the Tukey Method and 95% Confidence

Items Threshold	N	Mean	Grouping
1	30	5.538	A
2	30	5.382	A
3	30	5.291	A B
4	30	4.707	B C
6	30	4.566	C
5	30	4.279	C

Means that do not share a letter are significantly different.

Figure 32. Multiple Comparison Test on System Time vs. Num. of Items Threshold (High-Traffic Volume Distribution)

Figure 33 displays the interval plot of the system time for the scenarios of the medium-traffic volume distribution. Similar to the plot for the high-traffic volume distribution, the scenarios with thresholds of four, five and six items have the shortest mean system time. Moreover, the Tukey's pairwise comparison test in Figure *34* showed that there is no statistical difference among the system time of these scenarios. In addition, scenarios with thresholds of one, two and three items result in a statistically longer system time than the scenario of the current configuration. Therefore, for a medium-traffic volume distribution, setting a threshold on the number of items to direct passengers to the circulating conveyor lane, does not improve the performance of the checkpoint in terms of the mean system time.

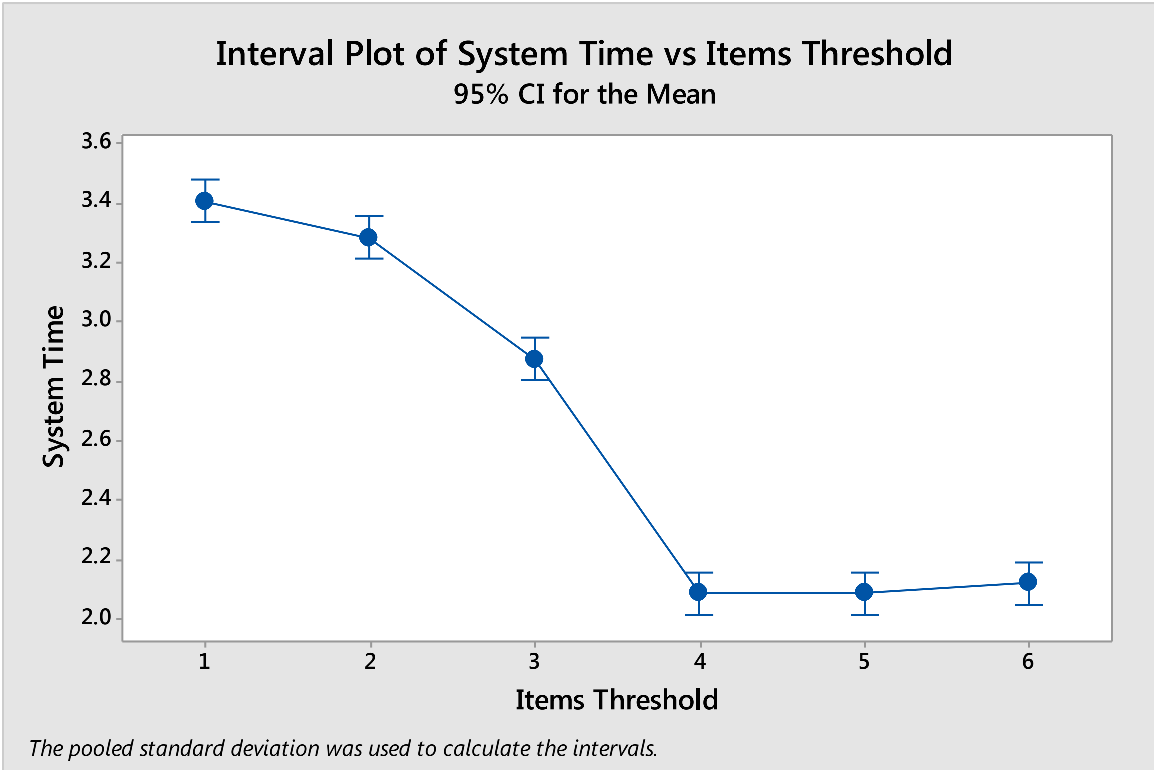

Figure 33. Interval Plot on System Time vs. Num. of Items Threshold (Medium-Traffic Volume Distribution)

Tukey Pairwise Comparisons

Grouping Information Using the Tukey Method and 95% Confidence

Items Threshold	N	Mean	Grouping
1	30	3.4077	A
2	30	3.2836	A
3	30	2.8743	B
6	30	2.1200	C
4	30	2.0869	C
5	30	2.0857	C

Means that do not share a letter are significantly different.

Figure 34. Multiple Comparison Test on System Time vs. Num. of Items Threshold (Medium-Traffic Volume Distribution)

Lastly, Figure 35 displays the interval plot of the system time for the low-traffic volume distribution. Different from the previous two cases, the minimum mean system time is among the scenarios with thresholds of three, four, five and six items.

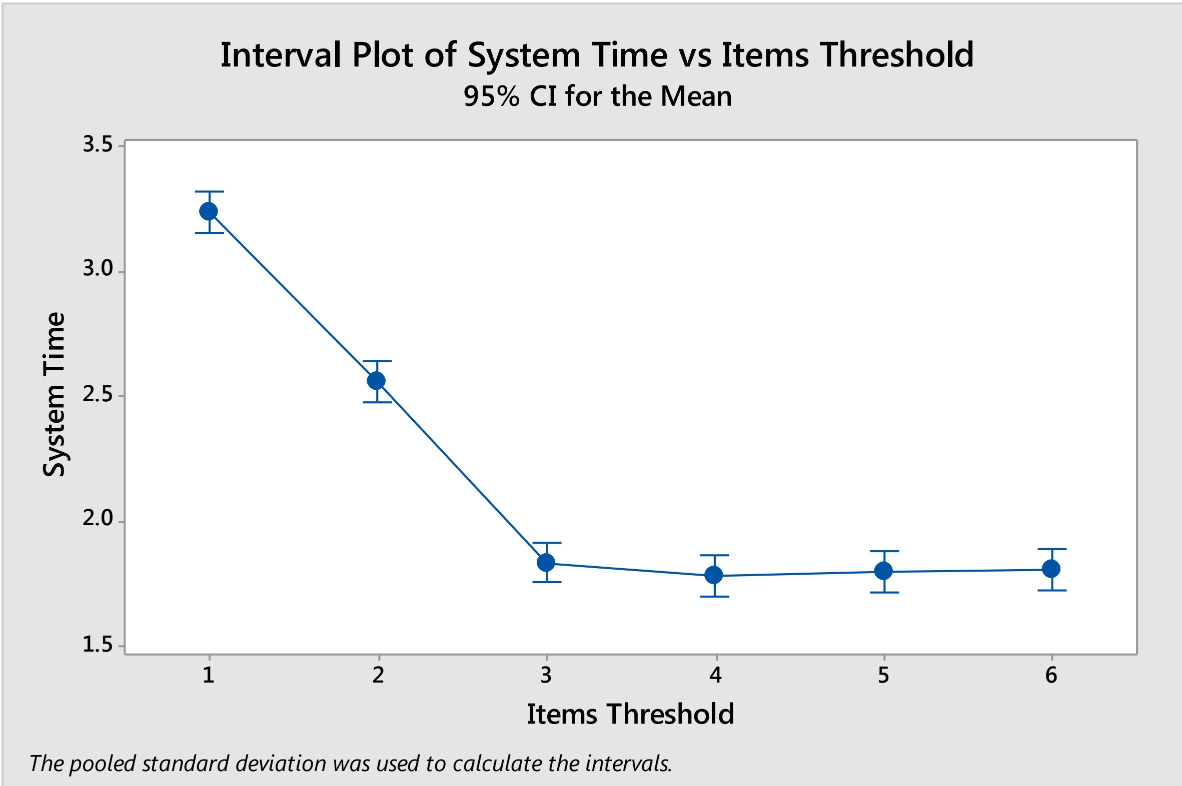

Figure 35. Interval Plot on System Time vs. Num. of Items Threshold
(Low-Traffic Volume Distribution)

Figure 36 displays the results from simultaneously comparing the mean system times of the six scenarios for the low-traffic volume distribution. As expected from the plot in Figure *35*, there is no significant difference among the mean system times of the scenarios with thresholds of three, four, five and six items. In addition, the scenarios with thresholds of one and two items result in statistically different mean system times than the rest of the scenarios, but their mean system times are longer. Therefore, similar to the results for the other two distributions, using a threshold to direct passengers to the lanes based on the number of items they carry, does not reduce significantly the mean system time for the low-traffic volume distribution.

Tukey Pairwise Comparisons

Grouping Information Using the Tukey Method and 95% Confidence

Items Threshold	N	Mean	Grouping
1	30	3.2443	A
2	30	2.5592	B
3	30	1.8360	C
6	30	1.8071	C
5	30	1.8012	C
4	30	1.7817	C

Means that do not share a letter are significantly different.

Figure 36. Multiple Comparison Test on System Time vs. Num. of Items Threshold (Low-Traffic Volume Distribution)

Replacing a Traditional Two Lane System with One Circulating Conveyor Lane

In most US airports, one of the major constraints for the design of security checkpoints is the space available to accommodate the continuously growing air passenger traffic. As a result, it is fundamental that any addition aiming to improve the performance of the checkpoints considers the least possible amount of space.

From the results in the first part of the experimentation, we found that the circulating conveyor significantly reduces the passengers' waiting time in the lines. In fact, replacing one traditional lane with one circulating conveyor lane as in the first prototype, reduced the mean system time of the base configuration by over 70%, as we could see in the analysis of variance in Figure 43. Nonetheless, the experimentation of this analysis was made under an arrival rate of 300 pph, which is significantly higher than the arrival rate for which a two-lane system is currently designed. This made us consider examining the possibility of replacing a complete two-lane system with one circulating conveyor lane system. This would allow the TSA to achieve comparable performance levels with a system requiring less space. Therefore, we used this experimentation section to determine the arrival rates for which the performance of one circulating conveyor lane is equivalent to that of a traditional two-lane system.

Three different versions of the simulation models were used for this part of the experimentation: the base model, featuring two traditional lanes; a separate model having one traditional lane only; and another model, featuring a single-circulating-conveyor lane. This would allow examining how the single-circulating-conveyor lane competes with the base configuration and with a single traditional lane.

The experiment consisted of analyzing the response of three performance measures to the change in arrival rates in each of the three models. The performance measures included the total system time, the passenger throughput from the AIT, and the probability that the time to composure, defined in the system definition section, is less than 10 minutes. We used eight different arrival rates ranging from 150 pph to 200 pph. For each arrival rate, we obtained 35 observations of each performance measure. These observations were used to construct the plots in Figure 37, Figure 38 and Figure 39. Each plot displays the mean response to the change in arrival rate of one of the three performance measures.

Figure *37* displays the mean response to the change in arrival rates for the AIT passenger throughput. Each series in the plot displays the response of the variable in one of the three simulation models. As we can see, with arrival rates under 180 pph, the AIT throughput of the single-circulating-conveyor-lane model is not significantly different from that of the base model (p-value > 0.143). On the other hand, the throughput of the model featuring one traditional lane is significantly lower than the throughputs of the two other models, even at an arrival rate of 150 pph. Only over 50% of the passengers are able to pass through the AIT when the arrival rate is 200 pph.

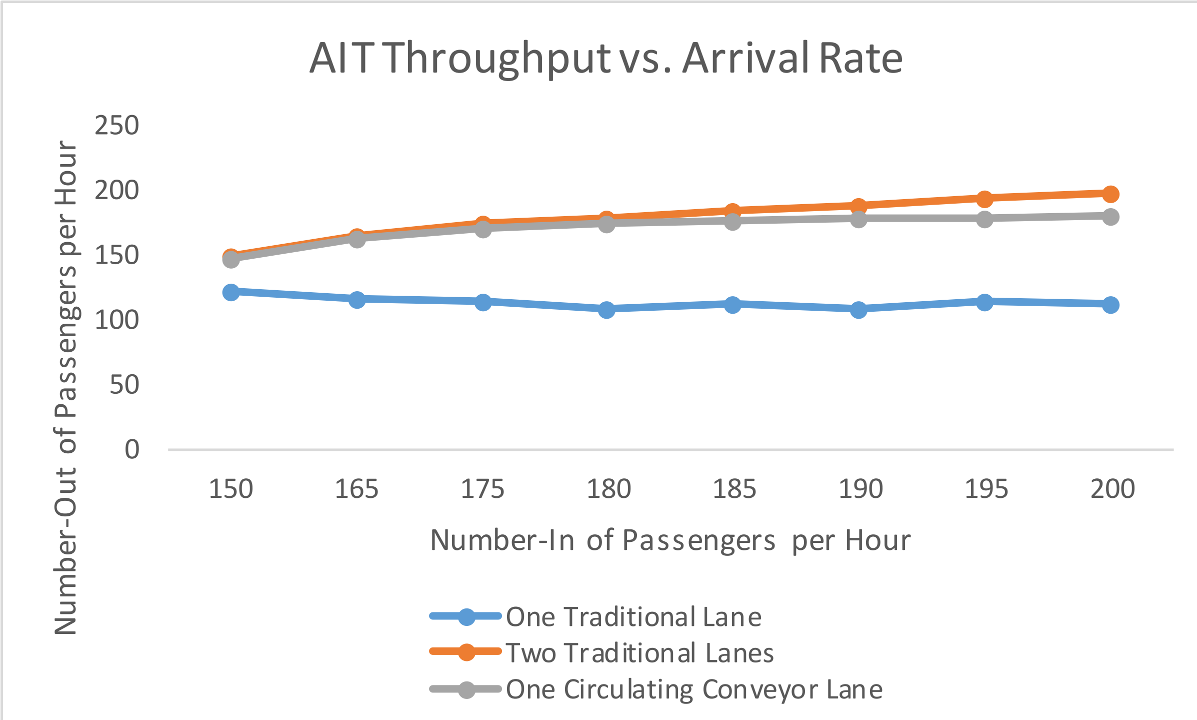

Figure 37. AIT Throughput vs. Arrival Rate

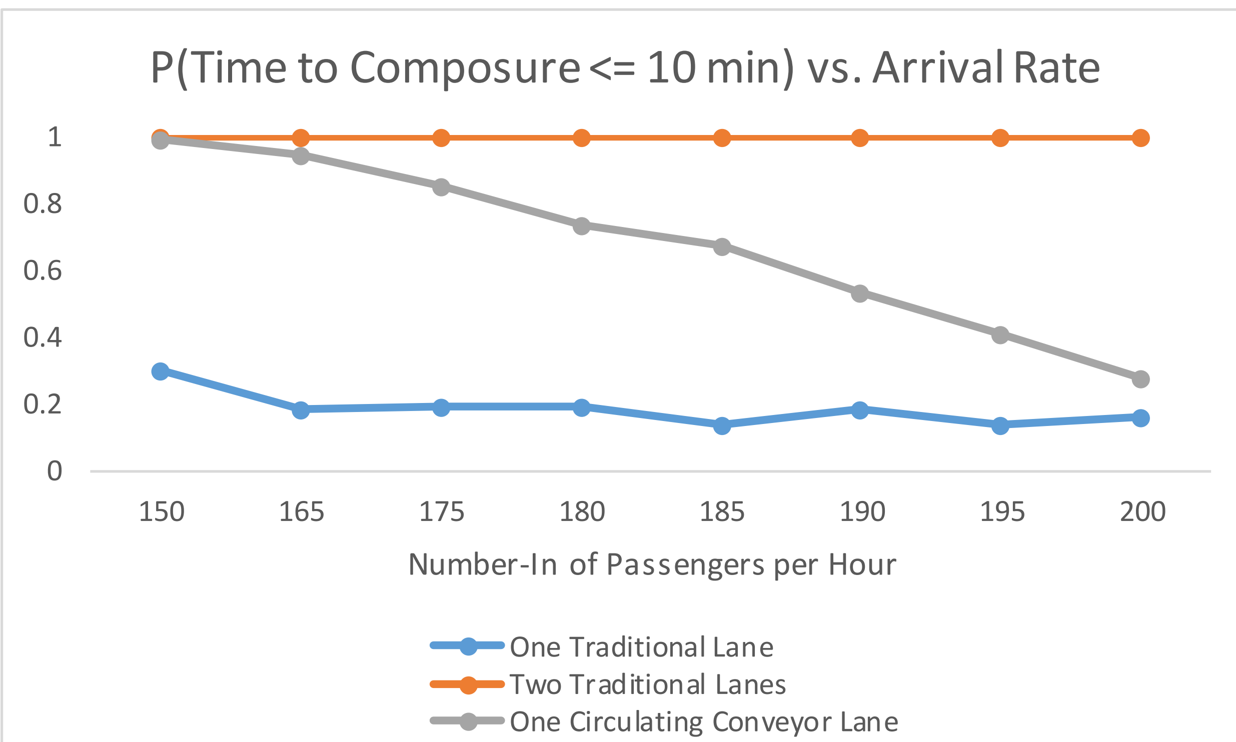

Figure 38. Prob. Time to Composure Less Than 10 min. vs. Arrival Rate

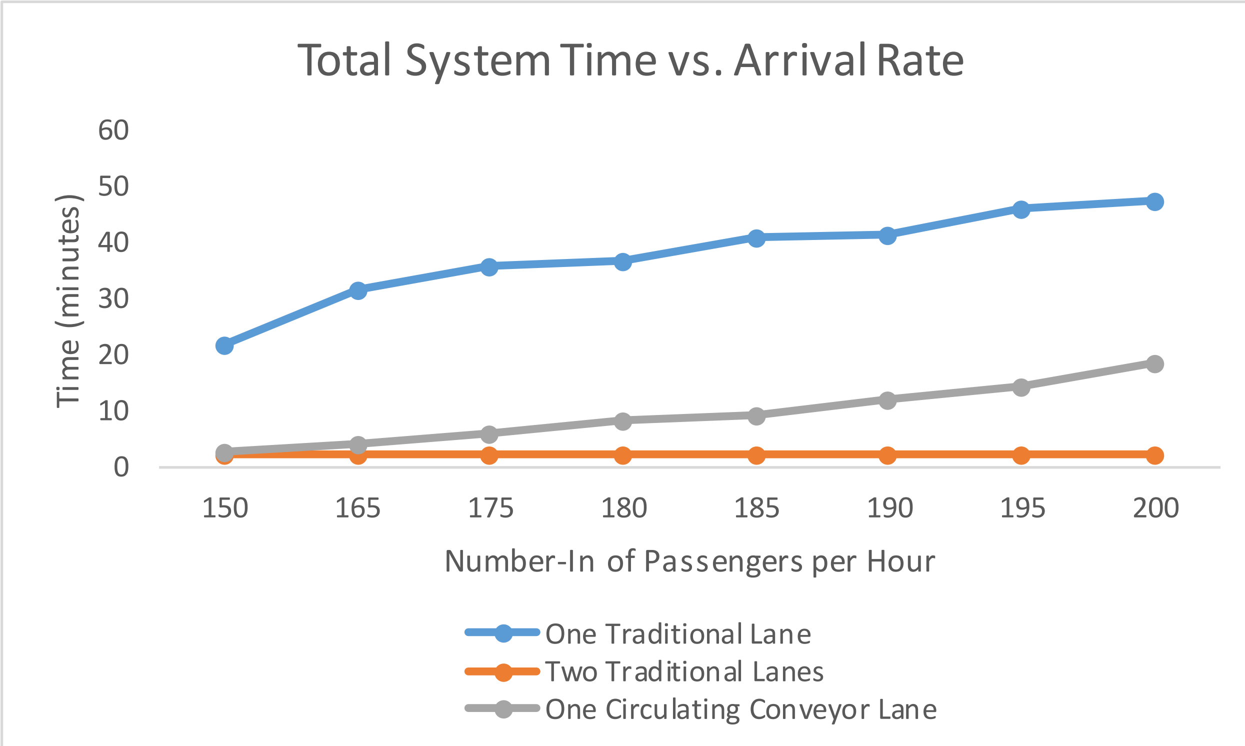

Figure 39. Total System Time vs. Arrival Rate

Figure 38 displays the mean response for the probability that the passengers' time to composure is less than 10 minutes. The mean difference between the responses of the base model and the model featuring the single circulating conveyor is essentially the same only at arrival rates under 150 pph (p-value = 0.083). However, the response for the model of the single circulating conveyor lane is over 70% at an arrival rate of 180 pph, while the mean throughput is statistically the same as in the base model. In other words, at an arrival rate of 180 pph, we could replace the two-traditional-lane system for one circulating conveyor lane, and obtain a statistically equivalent throughput with 70% of the passengers having a time to composure under 10 minutes. On the other hand, for the model featuring one traditional lane, the mean response is under 35% even at an arrival rate as low as 150 pph.

Figure 39 displays the mean response of the total system time of passengers. For the model featuring the single-circulating- conveyor lane, the mean system time is under 10 minutes for arrival rates under 185 pph. Nonetheless, for arrival rates ranging from 185 pph to 200 pph, the mean system time remains under 20 minutes. On the other hand, for the one-traditional-lane system, the system time is over 20 minutes when the arrival rate is 150 pph, and it reaches over 45 minutes when the arrival rate is 200 pph.

Therefore, the single-circulating conveyor lane clearly outperforms the single-traditional –lane system. On the other hand, whether the single-circulating-conveyor lane could replace a traditional two-lane system depends on the decision maker's tolerance level with respect to the checkpoint performance. For instance, if the decision maker is willing to accept an 85% probability that the time to composure is less than 10 minutes, the single-circulating-conveyor-lane system can replace the base model, and achieve the same throughput performance with arrival rates under 175 pph.

CONCLUSION AND FUTURE WORK

In a previous effort (Janer and Rossetti 2016), we found that replacing the exit roller for a circulating conveyor could increase the processing rate of passengers through the checkpoints by 28%. This study consisted of examining the effect of this circulating conveyor on the secondary screening process, as this element of the checkpoint was not considered previously. In addition, for a two-lane system where one lane features the traditional exit roller while the other lane features the circulating conveyor, we evaluated whether there could be any improvements in the passengers' system time from directing the passengers to the lanes based on the number of items they carry. Moreover, we examined the arrival rates for which a single circulating conveyor lane could achieve equivalent performance to that of a traditional two-lane system.

Three simulation models were developed for this study. The base model represented the current configuration, where items coming from the x-ray are delivered to an exit roller in both lanes of a mirror-two-lane system. The second model corresponds to the first prototype. This is also a two-lane system, but one lane features the traditional exit roller while the other lane features the circulating conveyor. The third model corresponds to the second prototype. This is a mirror-two-lane system, where the two lanes feature the circulating conveyor at the composure area.

In the first part of the experimentation, using an analysis of variance on the x-ray processing limit, we found that a limit of 15 seconds results in a shorter system time than a limit of 30 seconds and a limit of 7 seconds. Nonetheless, limits of 30 and 45 seconds result in essentially the same mean system time. Note the system time for the first portion of the experimentation did not include the time in secondary screening. To find the limit resulting in the minimum system time, we fitted a univariate response curve to 176 observations of the system time under different limits. We found that the critical point of the curve resulting in the minimum system time was 18 seconds. Sensitivity analysis was performed on this optimum limit using the coefficient of variation of the secondary screening distribution and the prototypes models. Although we did not construct a confidence interval on the optimum limit, it seemed that increasing the coefficient of variation of the secondary screening distribution resulted in a smaller optimum limit. In other words, reducing the mean of the distribution reduced the risk associated with failing to identify a threat, because the optimum limit was smaller. A smaller optimum limit increases the probability that an item requires secondary screening. Future work of this study should include developing confidence intervals on the optimum limits obtained from optimizing the univariate response curves. Through an additional analysis of variance, we found that the mean of the secondary screening distribution does not have a significant effect on the system time when the limit is at the optimum level. In addition, the results from the sensitivity analysis on the optimum limit, using the first and seconds prototype models, showed that the prototypes do not have any effect on the optimum x-ray processing time limit. Nonetheless, the models significantly decreased the minimum system time under the optimum x-ray processing time limit of each model. The first prototype resulted in a mean system time 70% shorter than that of the base model, while the second prototype resulted a mean system time 16 % shorter than that of the first prototype.

For the second portion of the experimentation, we evaluated the effect of six different thresholds on the number of items used to direct passengers to the circulating conveyor lane in the first prototype. We used a Tukey's multiple comparison test to compare simultaneously the mean system time of passengers for the six different thresholds. Different from the first portion of the experimentation, the system time response for this portion included the secondary screening process. We repeated this analysis for three different distributions on the number of items per passengers, obtained from Paul et al. (2009). For the three distributions, we obtained that the minimum system time was among the scenarios with thresholds on four, five and six items. The latest corresponds to the current scenario, where passengers are directed to the lane having the least number of passengers in the divestiture area. The mean difference among the three best scenarios was not significant for any of the three distributions. Therefore, directing passengers to the circulating conveyor lane, using a threshold on the number of items per passenger, does not significantly reduce the mean system time.

For the last portion of the experimentation, we found that for arrival rates under 180 pph, the mean probability that the passengers' time to composure is under 10 minutes was 30% lower for a single circulating conveyor lane than for the traditional two-lane system. Nonetheless, the throughput was statistically the same for both models. In addition, the mean system time for the model featuring the single circulating conveyor lane was under 10 minutes. Thus, if the TSA is willing to tolerate a decrease in 30% in the probability that passengers have a time to composure within 10 minutes, they could replace the traditional two-lane system for a single circulating conveyor lane for checkpoints where the arrival per AIT is less or equal to 180 pph.

Future work on this study should consider developing response surfaces to optimize the key metrics of a checkpoint performance. Independent factors for this response surface analysis should include the three simulation models, and the distributions of the secondary screening process, the x-ray inspection time and the TDC process, as these are the checkpoint elements with the highest utilization in the current configuration and the two prototypes.

REFERENCES

Blalock, G., V. Kadiyali, and D. H. Simon. The Impact of Post-9 / 11 Airport Security Measures on the Demand for Air Travel. *Journal of Law and Economics*, Vol. 50, No. 4, 2007, pp. 31–755.

De Barros, A. G., and D. D. Tomber. Quantitative Analysis of Passenger and Baggage Security Screening at Airports. *Journal of Advanced Transportation*, Vol. 41, No. 2, 2007, pp 171–193.

Cahya, S., E. Del Castillo, and J. J. Peterson. Computation of Confidence Regions for Optimal Factor Levels in Constrained Response Surface Problems. Journal of Computational and Graphical Statistics, Vol. 13, No. 2, 2004, pp. 499-518.

De Lange, R., I. Samoilovich, and B. V. Der Rhee. Virtual Queuing at Airport Security Lanes. *European Journal of Operational Research*, Vol. 225, No. 1, 2013, pp 153–165.

DFW Planning Department. *Dallas/Fort Worth Security Checkpoints - Tiger Team 2005 - Improving Throughput*, July 2006. https://www.dfwairport.com/dfwucm1prd/groups/public/documents/webasset/p1_008154.pdf. Accessed January 17, 2017

Doran, D., S. Gokhale, and N. Lownes. Analytic Model of Screening Times at Airport Security Checkpoints. In *Transportation Research Record: Journal of the Transportation Research Board. No. 2400,* Transportation Research Board of the National Academies, Washington, D.C., 2013, pp 1–8.

Dorton, S. L., and D. Liu. Effects of Baggage Volume and Alarm Rate on Airport Security Screening Checkpoint Efficiency Using Queuing Networks and Discrete Event Simulation. *Human Factors and Ergonomics in Manufacturing*, Vol. 26, No. 1, 2016, pp 95–109.

Fayez, M.S., et al. Managing Airport Operations Using Simulation. *Journal of Simulation* Vol. 2, No.1, 2008, pp 41–52.

Guru, A., and P. Savory. A Template-Based Conceptual Modeling Infrastructure for Simulation of Physical Security Systems. *Proceedings of the 2004 Winter Simulation Conference,* 2004, pp 866-873.

Hobbs, B., M. D. Rossetti, P. Faas. (2006) An Object-Oriented Framework For Simulating Automatic Data Collection Systems, *The Proceedings of the 2006 Winter Simulation Conference,* L. F. Perrone, F. P. Wieland, J. Liu, B. G. Lawson, D. M. Nicol, and R. M. Fujimoto, eds., Piscataway, New Jersey: Institute of Electrical and Electronic Engineers

Leone, K., and R. Liu. Improving Airport Security Screening Checkpoint Operations in the US via Paced System Design. *Journal of Air Transport Management*, Vol. 17, No. 2, 2011, pp 62–67.

Nie, X., et al. Simulation-Based Selectee Lane Queueing Design for Passenger Checkpoint Screening. *European Journal of Operational Research,* Vol. 219, No. 1, 2012, pp 146–155.

Paul, J. A., et al. Airport Security System Design: Passenger Flow Analysis and Simulation Modeling. *Protecting Airline Passengers in the Age of Terrorism*, ABC- Clio, Santa Barbara, CA, 2009. Edited by Paul Seidenstat and Francis X. Splane.

Pendergraft, D. R., C. V. Robertson, and S. Shrader. Simulation of an Airport Passenger Security System. *Proceedings of the 2004 Winter Simulation Conference*, 2004, pp 874–878.

Price, H. *FAA Forecast Sees Continued, Steady Growth in Air Travel. Federal Aviation Administration*, March 2015.

Solomon, R. *TSA chief: Delta innovation lanes make 'dramatic improvements'*, June 2016. http://news.delta.com/tsa-chief-delta-innovation-lanes-make-dramatic-improvements.

TSA Pre-Check Expansion Act. Report of the Committee on Commerce, Science, and Transportation on H. R. 2843. 2016. https://www.congress.gov/bill/114th-congress/house-bill/2843/

Wan, F., et al. An Exact Confidence Set for a Maximum Point of a Univariate Polynomial Function in a given Interval. Technometrics, Vol. 57, No. 4, pp 559-565.

Wetter, O. E., M. Lipphardt, and F. Hofer. External and Internal Influences on the Security Control Process at Airports. *Proceedings – IEEE International Carnahan Conference on Security Technology*, 2010, pp 301–309.

Wilson, D., E. K. Roe, and S. A. So. Security Checkpoint Optimizer (SCO): An Application for Simulating the Operations of Airport Security Checkpoints. *Proceedings of the 2006 Winter Simulation Conference*, 2006, pp 529–535.

APPENDIX

One-way ANOVA: ST No 2ndScreening versus XRay PT Limit

Method

Null hypothesis	All means are equal
Alternative hypothesis	At least one mean is different
Significance level	α = 0.05

Equal variances were assumed for the analysis.

Factor Information

Factor	Levels	Values
XRay PT Limit	3	15, 30, 45

Analysis of Variance

Source	DF	Adj SS	Adj MS	F-Value	P-Value
XRay PT Limit	2	28.85	14.425	12.02	0.000
Error	21	25.20	1.200		
Total	23	54.05			

Model Summary

S	R-sq	R-sq(adj)	R-sq(pred)
1.09547	53.37%	48.93%	39.10%

Means

XRay PT Limit	N	Mean	StDev	95% CI
15	8	20.145	0.667	(19.339, 20.950)
30	8	22.441	1.210	(21.635, 23.246)
45	8	22.499	1.300	(21.693, 23.304)

Pooled StDev = 1.09547

Figure 40. ANOVA on System Time vs. X-ray PT Limit Levels (Base Model and CV = 0.71)

Tukey Pairwise Comparisons

Grouping Information Using the Tukey Method and 95% Confidence

XRay PT Limit	N	Mean	Grouping
45	8	22.499	A
30	8	22.441	A
15	8	20.145	B

Means that do not share a letter are significantly different.

Figure 41. Multiple Comparisons on System Time vs. X-ray PT Limit Levels
(Base Model and CV = 0.71)

Table 7. Statistical Significance of Regression in Figure 22

Regression Statistics	
Multiple R	0.995
R Square	0.990
Adjusted R Square	0.990
Standard Error	2.926
Observations	176

ANOVA

	df	*SS*	*MS*	*F*	*Significance F*
Regression	4	150017.1	37504.3	4379.5	0.0
Residual	171	1464.4	8.6		
Total	175	151481.4			

	Coefficients	*Standard Error*	*t Stat*	*P-value*
Intercept	-238.8	26.7	-9.0	0.0
X Variable 1	120.0	7.4	16.1	0.0
X Variable 2	-14.1	0.7	-19.0	0.0
X Variable 3	0.6	0.0	20.1	0.0
X Variable 4	0.0	0.0	-20.2	0.0

Table 8. Statistical Significance of Regression in Figure 23

Regression Statistics	
Multiple R	0.990
R Square	0.980
Adjusted R Square	0.980
Standard Error	2.760
Observations	176

ANOVA

	df	*SS*	*MS*	*F*	*Significance F*
Regression	3	64270.0	21423.3	2811.7	0.0
Residual	172	1310.5	7.6		
Total	175	65580.5			

	Coefficients	*Standard Error*	*t Stat*	*P-value*
Intercept	376.4	7.5	50.3	0.0
X Variable 1	-56.9	1.5	-37.1	0.0
X Variable 2	3.0	0.1	30.0	0.0
X Variable 3	-0.1	0.0	-24.9	0.0

Table 9. Statistical Significance of Regression in Figure 17

Regression Statistics	
Multiple R	0.993
R Square	0.986
Adjusted R Square	0.985
Standard Error	1.660
Observations	176.000

ANOVA

	df	*SS*	*MS*	*F*	*Significance F*
Regression	4	32368.0	8092.0	2934.9	0.0
Residual	171	471.5	2.8		
Total	175	32839.5			

	Coefficients	*Standard Error*	*t Stat*	*P-value*
Intercept	450.0	15.1	29.7	0.0
X Variable 1	-88.6	4.2	-21.0	0.0
X Variable 2	6.7	0.4	16.0	0.0
X Variable 3	-0.2	0.0	-12.4	0.0
X Variable 4	0.0	0.0	9.9	0.0

One-way ANOVA: ST under Optimum Limit versus CV

```
Method

Null hypothesis         All means are equal
Alternative hypothesis  At least one mean is different
Significance level      α = 0.05

Equal variances were assumed for the analysis.

Factor Information
Factor  Levels  Values
CV           3  0.5, 1.0, 1.5

Analysis of Variance
Source   DF   Adj SS   Adj MS  F-Value  P-Value
CV        2    14.89    7.444     0.31    0.736
Error   102  2467.83   24.194
Total   104  2482.72

Model Summary
      S   R-sq  R-sq(adj)  R-sq(pred)
4.91878  0.60%      0.00%       0.00%

Means
CV    N    Mean  StDev       95% CI
0.5  35  20.811  5.355  (19.162, 22.460)
1.0  35  19.988  5.435  (18.339, 21.637)
1.5  35  20.038  3.790  (18.389, 21.688)
Pooled StDev = 4.91878
```

Figure 42. ANOVA on System Time vs. Coefficient of Variation
(Base Model and Optimum X-Ray PT Limit)

Table 10. Significance of Regression Model in Figure 27Figure 27. Response Curve for Prototype 1 Model (CV = 0.71)

Regression Statistics	
Multiple R	0.9957
R Square	0.9913
Adjusted R Square	0.9911
Standard Error	2.9994
Observations	176

ANOVA

	df	*SS*	*MS*	*F*	*Significance F*
Regression	4	175724.3	43931.1	4883.1	0.0
Residual	171	1538.4	9.0		
Total	175	177262.7			

	Coefficients	*Standard Error*	*t Stat*	*P-value*
Intercept	-111.49	27.34	-4.08	0.00
X Variable 1	87.90	7.61	11.54	0.00
X Variable 2	-11.51	0.76	-15.17	0.00
X Variable 3	0.54	0.03	16.85	0.00
X Variable 4	-0.01	0.00	-17.49	0.00

Table 11. Significance of Regression in Figure 28**Error! Reference source not found.**

Regression Statistics	
Multiple R	0.9935
R Square	0.9870
Adjusted R Square	0.9867
Standard Error	3.8891
Observations	176

ANOVA

	df	*SS*	*MS*	*F*	*Significance F*
Regression	4	195785.9	48946.5	3236.1	0.0
Residual	171	2586.4	15.1		
Total	175	198372.3			

	Coefficients	*Standard Error*	*t Stat*	*P-value*
Intercept	-160.22	35.45	-4.52	0.00
X Variable 1	104.19	9.87	10.55	0.00
X Variable 2	-13.34	0.98	-13.55	0.00
X Variable 3	0.63	0.04	14.96	0.00
X Variable 4	-0.01	0.00	-15.51	0.00

One-way ANOVA: System Time versus Model

```
Method

Null hypothesis         All means are equal
Alternative hypothesis  At least one mean is differen
Significance level      α = 0.05

Equal variances were assumed for the analysis.

Factor Information
Factor  Levels  Values
Model        3  Base Model, Prototype 1, Prototype 2

Analysis of Variance

Source   DF  Adj SS   Adj MS  F-Value  P-Value
Model     2  7373.2  3686.59   413.76    0.000
Error   102   908.8     8.91
Total   104  8282.0

Model Summary

      S    R-sq  R-sq(adj)  R-sq(pred)
2.98494  89.03%     88.81%      88.37%

Means

Model         N    Mean   StDev        95% CI
Base Model   35  20.679   4.885  (19.679, 21.680)
Prototype 1  35   4.072   1.672  ( 3.071,  5.073)
Prototype 2  35  1.9285  0.2741  (0.9278, 2.9293)

Pooled StDev = 2.98494
```

Figure 43. ANOVA on System Time vs. Models (CV = 0.71 and Optimum X-Ray PT Limit)

Tukey Pairwise Comparisons

```
Grouping Information Using the Tukey Method and 95% Confidence

Model         N    Mean  Grouping
Base Model   35  20.679  A
Prototype 1  35   4.072    B
Prototype 2  35  1.9285      C

Means that do not share a letter are significantly different.
```

Figure 44. Multiple Comparison Test on System Time vs. Models
(CV = 0.71 and Optimum X-Ray PT Limit)